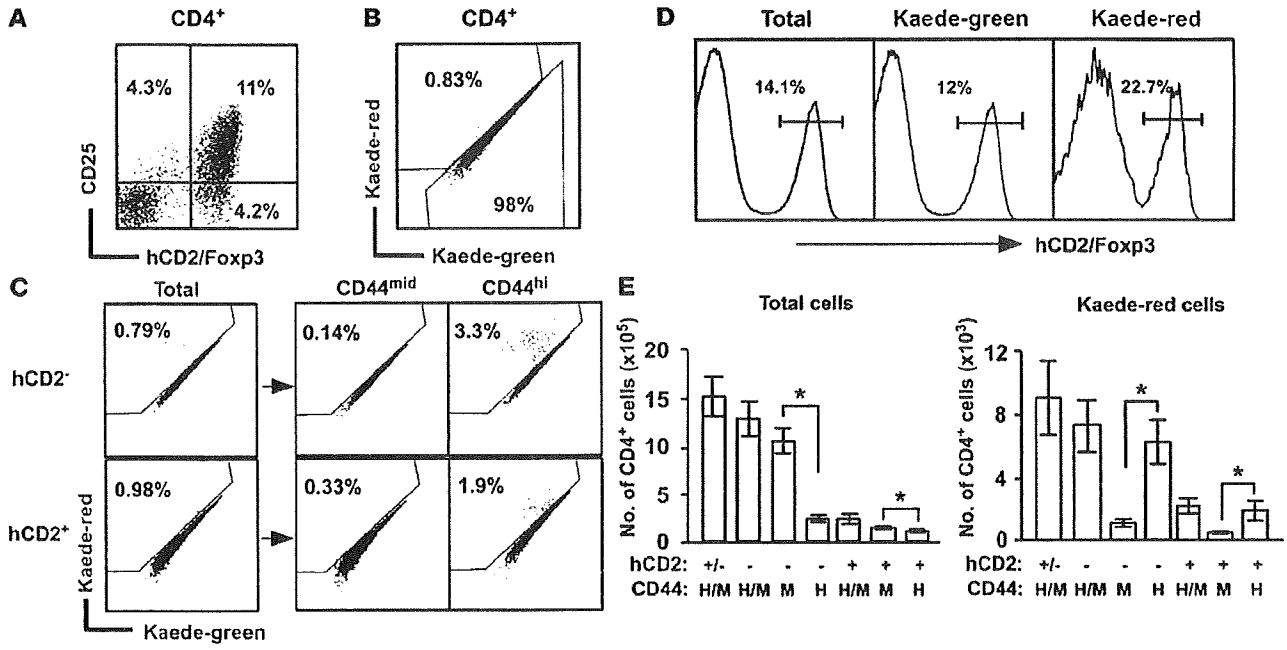

Figure 2

Migration of Tregs from the skin to DLNs. (**A**–**E**) The DLN cells of Kaede/Foxp3$^{hCD2/hCD52}$ mice photoconverted on the abdomen 24 hours prior were stained with CD4, CD25, and hCD2 mAbs. Shown here are the flow cytometric plots for hCD2/Foxp3 and CD25 staining among CD4$^+$ cells (**A**) and Kaede-red and Kaede-green expression on hCD2$^+$CD4$^+$ cells among skin DLN cells (**B**). (**C**) The DLNs and non-DLNs from the mice 24 hours after photoconversion were stained with CD4, hCD2, and CD44 mAbs and subjected to flow cytometry. (**D**) hCD2/Foxp3 expression in total (Kaede-red plus Kaede-green), Kaede-red, and Kaede-green CD4 cells was compared by flow cytometry. (**E**) The numbers of CD44^{mid} naive (M), CD44^{hi} memory (H), and naive plus memory (H/M) phenotypes of hCD2$^-$CD4$^+$ non-Tregs (–), hCD2$^+$CD4$^+$ Tregs (+), and total (hCD2$^-$ and hCD2$^+$; +/–) CD4$^+$ T cells in total CD4$^+$ (Kaede-red plus Kaede-green) cells and Kaede-red cells in the DLNs were counted. Data are presented as means ± SD and are representative of 3 independent experiments. Student's *t* test was performed between the indicated groups. $^*P < 0.05$. Numbers within plots or histograms indicate percentage of cells in the respective areas (**A**–**D**).

Treg migration from the skin during a cutaneous immune reaction. We tracked the extent of CD4$^+$ T cell migration from the skin during an immune response and sought to evaluate the role of CD4$^+$ T cells migrating from the skin. The dorsal skin of Kaede/Foxp3$^{hCD2/hCD52}$ mice was sensitized with 2,4-dinitro-1-fluorobenzene (DNFB), and 5 days later, the abdominal skin was challenged with DNFB. Two days after challenge, the abdominal skin was exposed to violet light for photoconversion, and another 24 hours later, the draining axillary LN cells were analyzed by flow cytometry (Figure 3A). The frequency of Kaede-red cells among CD4$^+$ T cells in the DLNs was increased up to 3% (Figure 3B) from that in the steady state (0.83%; Figure 2B). In addition, although 21% of total CD4$^+$ cells were Tregs, the number of hCD2$^+$ Tregs became comparable to that of non-Tregs in Kaede-red phenotype (49%; Figure 3, C and D). Again, the CD44^{hi} memory cells were major migrants from the challenged skin similarly to the steady state (Figure 3D and Figure 2E). The number of total CD4$^+$ T cells in DLN increased by 3-fold during contact hypersensitivity (CHS) compared with that in the steady state. However, the number of Kaede-red migratory non-Tregs and Tregs during CHS increased more drastically, by about 10- and 20-fold, respectively (Figure 2E and Figure 3D).

Consistent with increase of CD4$^+$ T cells migrating from the challenged skin into DLN, the numbers of both CD4$^+$ Tregs and CD4$^+$ non-Tregs were elevated when mice were sensitized and challenged compared with the steady state, and the ratio of Tregs to CD4$^+$ T cells during the immune response became higher than that in the steady state (Figure 3E). These results suggest that more Tregs than non-Tregs accumulate in the skin during the cutaneous immune response.

It is known that cutaneous dendritic cells migrate into the DLNs in a CCR7-dependent manner (20) and that in humans, most circulating Tregs express skin-homing receptors and CCR7 (21). To address whether skin T cells have the potential to migrate into the regional LNs, skin cell suspensions were obtained from the ears of mice sensitized on the abdomen and challenged on the ear with DNFB and applied to a transwell assay. The Tregs showed good chemotactic responses to CCL21 comparable to that of MHC class II$^+$ cutaneous dendritic cells (Figure 3F). Similar chemotactic activity to CCL21 was seen in CD4$^+$ non-Tregs (data not shown). Since the ratio of Tregs and non-Tregs in Kaede-red CD4$^+$ T cells in LNs was comparable to that in the skin at the time of photoconversion, Tregs and non-Tregs in the skin seem to have equivalent propensity to migrate to the DLN. In addition, we evaluated the CCR7 expression of Tregs in the skin before and after challenge and found that Tregs in the skin expressed CCR7 both before and after challenge and that the expression level of CCR7 of Tregs after challenge was slightly lower than that before challenge (Supplemental Figure 5).

Role of Tregs in the elicitation phase of CHS. As shown above, Tregs accumulate in the skin and they have the capacity to migrate to DLNs during the CHS response. These results prompted us to

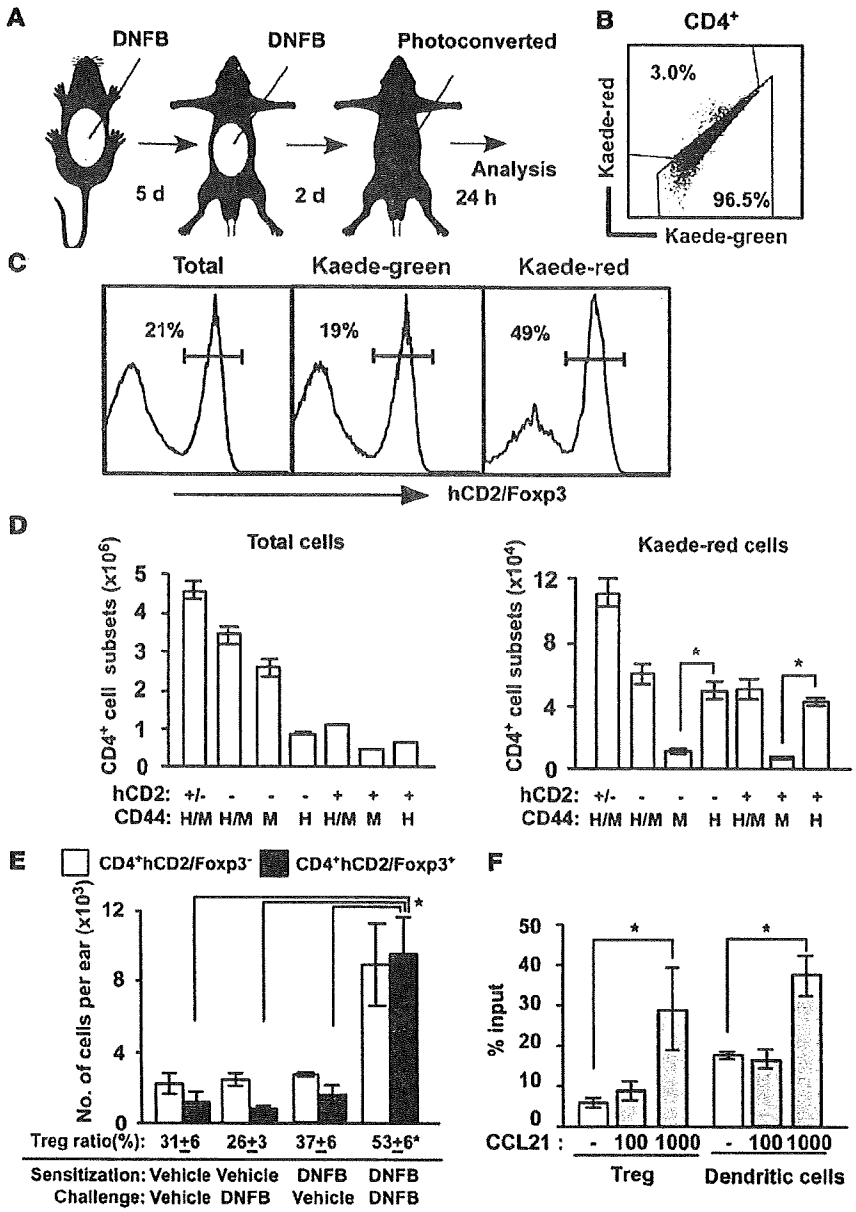

Figure 3

Cell migration from the skin to DLN during a cutaneous immune response. (**A**) Scheme of the experimental protocol is as follows: the dorsal skin of Kaede/Foxp3$^{hCD2/hCD52}$ was sensitized, and 5 days thereafter the abdominal skin was challenged. 2 days after challenge, the painted areas were photoconverted, and 24 hours after photoconversion, cells from the skin DLNs were analyzed by flow cytometry. (**B** and **C**) The frequency of Kaede-red and Kaede-green cells among CD4$^+$ cells, and the frequencies of hCD2/Foxp3+ cells in total, Kaede-green, and Kaede-red cells among CD4$^+$ cells were analyzed. Numbers within plots or histograms indicate percentage of cells in the respective areas. (**D**) The numbers of CD44^{mid} naive (M), CD44^{hi} memory (H), and naive plus memory (H/M) phenotypes of hCD2$^-$CD4$^+$ non-Tregs (–), hCD2$^+$CD4$^+$ Tregs (+), and total (hCD2$^-$ and hCD2$^+$; +/–) CD4$^+$ T cells among total CD4$^+$ cells and Kaede-red cells in the DLNs were counted. (**E**) Number of Tregs and non-Tregs in the skin. The mice were painted with DNFB or vehicle on the abdomen, followed by DNFB or vehicle application on the ears. The number of CD4$^+$ Tregs and CD4$^+$ non-Tregs and the percentage ratio of Tregs among CD4$^+$ T cells in the ears were measured. (**F**) Transwell assay. The number of hCD2$^+$CD4$^+$ cells and CD11c$^+$ cells of skin-cell suspensions from Foxp3$^{hCD2/hCD52}$ mice that migrated to the lower chamber was analyzed. Data are presented as means ± SD (**D**–**F**) and are representative of 3 independent experiments. Student's *t* test was performed between the indicated groups. $^*P < 0.05$ (**D**–**F**).

evaluate the role of Tregs in the cutaneous immune response. In a murine CHS model, we found that administration of Campath-1G Ab (a depleting Ab for the human CD52 antigen; ref. 22) resulted in a marked decrease in the number of Tregs in the DLNs and the skin, 1–3 days after injection (Figure 4A and data not shown). Kaede/Foxp3$^{hCD2/hCD52}$ mice were sensitized with DNFB on the abdomen and treated in the presence or absence of Campath-1G Ab. The ear thickness changes after the challenge on the ears were significantly prolonged by the treatment with Campath-1G Ab at each time point compared with in control mice (Figure 4B). This enhancement of CHS response by Campath-1G Ab was not observed when C57BL/6 (B6) wild-type mice were used, which excluded the possibility of the nonspecific effect of Campath-1G Ab (Supplemental Figure 6). In addition, the ear thickness changes of mice treated with control rat IgG were comparable to those treated without Campath-1G Ab (data not shown). These results demonstrate that Tregs play an important role in the challenge phase in terminating the CHS response.

Suppressive activity of Kaede-red and Kaede-green Tregs on T cell proliferation. To further determine the suppressive function of the Tregs migrating from the skin during the cutaneous immune response, Kaede-red and Kaede-green CD4$^+$ Tregs in the skin DLN were prepared as in Figure 3A and cocultured with regional LN cells from DNFB-sensitized mice. Antigen-specific T cell proliferation induced by 2,4-dinitrobenzene sulfonic acid (DNBS), a water-soluble compound with the same antigenicity as DNFB, was significantly inhibited by addition of 6×10^3 Kaede-red Tregs (Figure 4C). On the other hand, 8 times the number of Kaede-green Tregs was required to achieve a similar magnitude of inhibitory effect of the Kaede-red Tregs (Figure 4C). These data indicate that the skin-

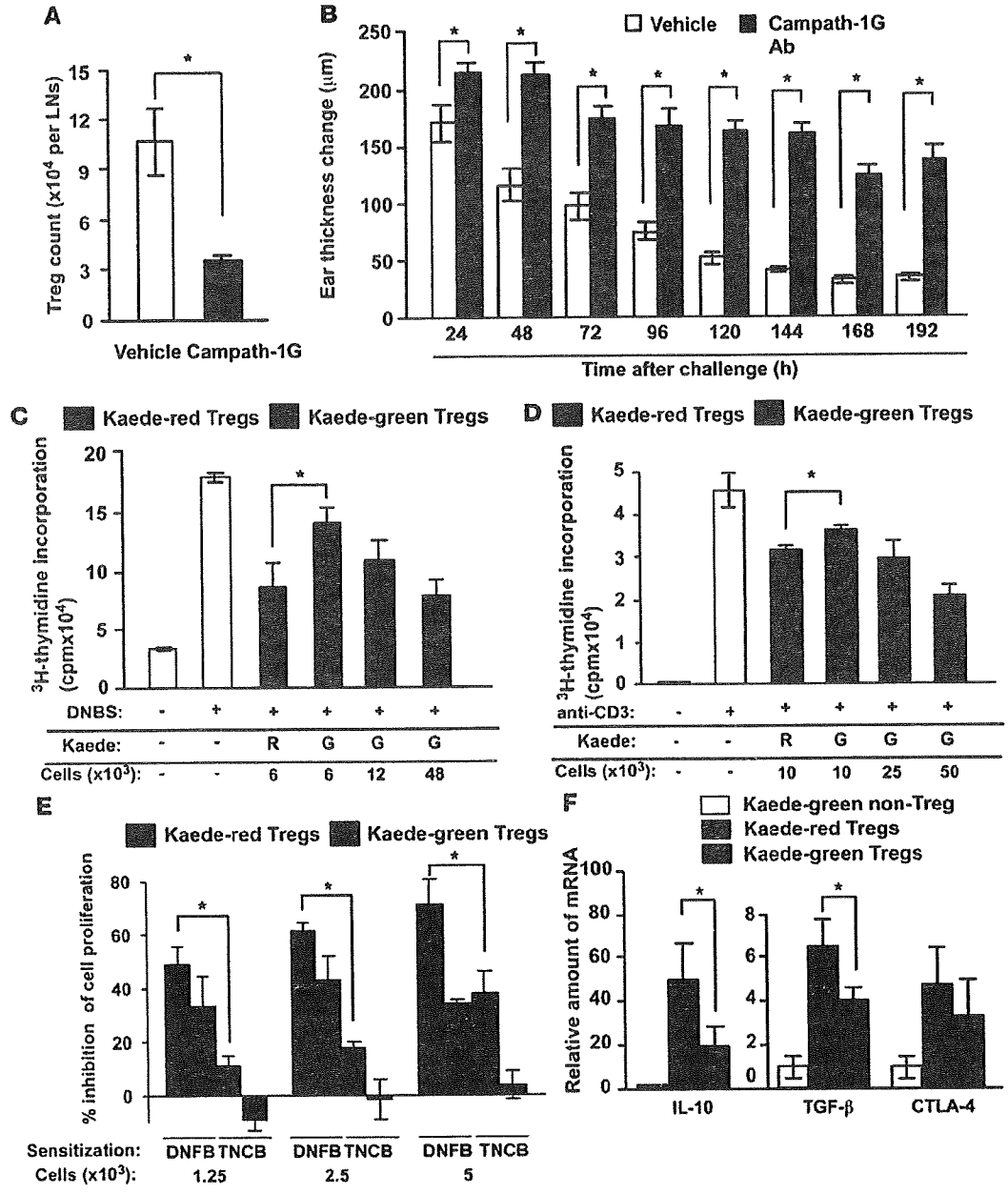

Figure 4

Enhanced ear swelling response by Treg depletion and immunosuppressive activity of Treg subsets on T cell proliferation in vitro. (**A**) The number of Tregs in the LNs after administration of Campath-1G Ab. (**B**) CHS: the Kaede/Foxp3$^{hCD2/hCD52}$ mice were sensitized, and injected with vehicle or Campath-1G Ab before challenge (n = 8 for each group). (**C**–**F**) Immunosuppressive activity of Tregs. Kaede-red and Kaede-green Tregs were sorted from the Kaede/Foxp3$^{hCD2/hCD52}$ mice, sensitized, challenged, and photoconverted. (**C**) Skin DLN cells of mice sensitized with DNFB were stimulated with DNBS in the presence or absence of Kaede-red Tregs or Kaede-green Tregs in vitro (n = 3). (**D**) Suppressive effect of Tregs in vitro. Kaede-red and Kaede-green Tregs were prepared as above and added to T cells stimulated with plate-bound anti-CD3 Ab. (**E**) Antigen specificity of Treg functions. LN cells from DNFB-sensitized or TNCB-sensitized mice were stimulated with DNBS or TNBS in vitro. Kaede-red and Kaede-green Tregs were added, and percentage inhibition of cell proliferation was evaluated as follows: (cell proliferation with DNBS or TNBS) – (cell proliferation with DNBS or TNBS in the presence of Tregs)/(cell proliferation with DNBS or TNBS) – (cell proliferation with vehicle) x 100. (**F**) Quantitative RT-PCR analysis on mRNA for *Il10* (IL-10), *Tgfb1* (TGF-β), and *Ctla4* (CTLA-4) of Kaede-red Tregs and Kaede-green Tregs. The expression of each gene was normalized by the expression of *Gapdh*, and those in Kaede-green non-Tregs were normalized to 1 (n = 3). Data are representative of 3 independent experiments and presented as means ± SD (**A**–**F**). *$P < 0.05$ between the indicated groups (Student's t test, **A**, **B**, **E**, and **F**; 1-way ANOVA followed by Dunnett multiple comparison test, **C** and **D**).

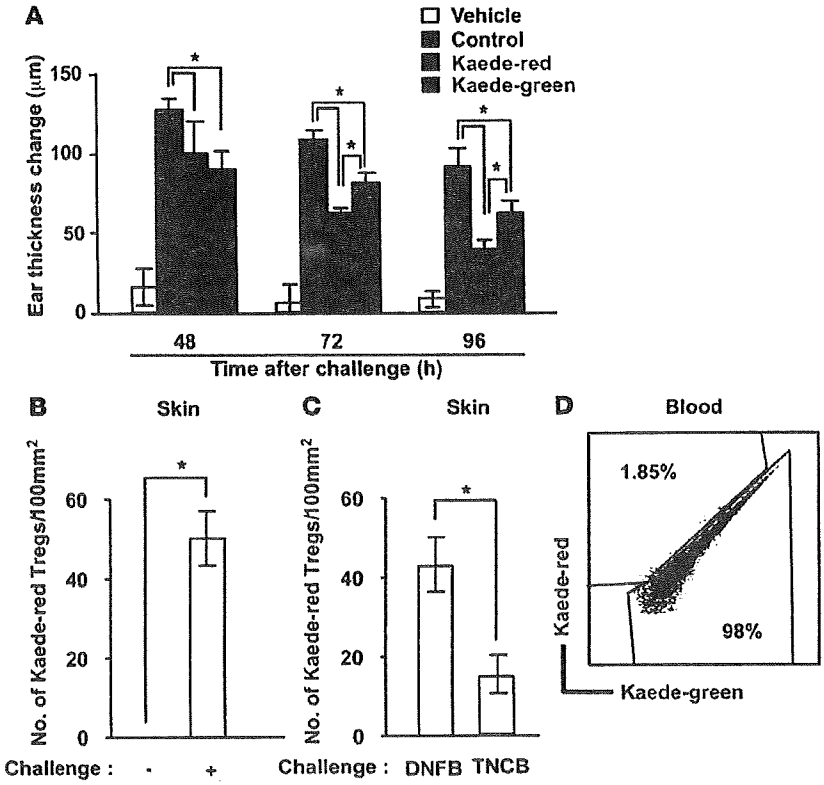

Figure 5

Immunosuppressive effect of Kaede-red Tregs in the skin. (**A**) Suppression of CHS response by Kaede-red Tregs. Kaede-red or Kaede-green Tregs (4×10^3 cells/ear) of Kaede/Foxp3$^{hCD2/hCD52}$ mice sensitized, challenged, and photoconverted as in Figure 3A were injected into ear skin of mice sensitized with DNFB 5 days prior. Immediately after injection, the mice were challenged, and the ear thickness change was measured at 48, 72, and 96 hours after challenge. (**B–D**) The mice were sensitized, challenged, and photoconverted as in Figure 3A. Twenty-four hours after photoconversion, 20 μl of 0.3% DNFB (challenge; +) or vehicle (challenge; –) (**B**) or 20 μl of 0.3% DNFB or 20 μl of 1% TNCB (**C**) was painted onto the ear. Twenty-four hours later, the ear skin and blood (**D**) were collected and dissociated for flow cytometry. The number of Kaede-red Tregs in the skin and the frequency of Kaede-red Tregs in CD4$^+$ T cell subset of the blood were evaluated ($n = 3$, each group). Data are presented as means ± SD and representative of 3 independent experiments (**A–C**). Student's t test was performed between the indicated groups. $^*P < 0.05$. Numbers within plots indicate percentage of cells in the respective areas (**D**).

derived Tregs have a stronger inhibitory effect on hapten-specific T cell proliferation than LN-resident Tregs. It should be noted that we might underestimate the inhibitory capacity of skin-migratory T cells relative to resident Tregs, since Kaede-green cells should have included the cells migrated from the skin before photoconversion and the cells that infiltrated to the skin after photoconversion and migrated to DLN.

We tested the effect of the Tregs on antigen-nonspecific T cell proliferation stimulated with membrane-bound anti-CD3 Ab. Kaede-red Tregs inhibited T cell proliferation more potently than did Kaede-green Tregs, and again a higher number of Tregs were required (Figure 4D) to obtain an extent of inhibition similar to that seen in Figure 4C.

To further evaluate the antigen specificity of Tregs in T cell proliferation, we isolated the DLN cells 5 days after DNFB or 2,4,6-trinitro-l-chlorobenzene (TNCB) sensitization and restimulated them with DNBS or trinitrobenzene sulfonic acid (TNBS), respectively, and added Kaede-red Tregs or Kaede-green Tregs prepared from the DLNs as in Figure 3A. Kaede-red Tregs inhibited DNBS-induced T cell proliferation more than Kaede-green Tregs (Figure 4E), as shown in Figure 4C. However, this antiproliferative effect was not seen when these Kaede-red or Kaede-green Tregs were added to TNBS-stimulated LN cells from the mice sensitized with TNCB (Figure 4E). In addition, in the criss-cross comparison, similar antigen-specificity was observed on TNCB-immunized Kaede-red Tregs (data not shown). We also analyzed mRNA expressions of inhibitory cytokines and surface molecules by quantitative RT-PCR. Kaede-red Tregs expressed higher mRNA levels of *Il10* and *Tgfb1* than Kaede-green Tregs (2, 3, 23) (Figure 4F). On the other hand, although there was no significant difference, Kaede-red Tregs tended to express higher mRNA levels of cytotoxic T lymphocyte-associated molecule-4 (*Ctla4*) than did Kaede-green Tregs (2, 3, 23) (Figure 4F). These results suggest that Tregs migrating from the skin have a more efficient suppressive potency on T cell proliferation with abundant inhibitory mediators and that this antiproliferative effect shows some antigen specificity.

Tregs recirculating from the skin inhibit local cutaneous immune response in situ. The strong ability of Kaede-red Tregs to suppress in vitro T cell proliferation prompted us to determine whether Kaede-red Tregs can inhibit a local cutaneous immune response in situ. Kaede-red or Kaede-green Tregs prepared as described (Figure 3A) were injected subcutaneously into the ears of mice sensitized with DNFB 5 days before, and the ears were challenged with DNFB. The DNFB-induced ear thickness change was suppressed by the injection of Kaede-red and Kaede-green Tregs at all time points (Figure 5A). It was noted, however, that Kaede-red Tregs suppressed CHS more than Kaede-green Tregs at 72 and 96 hours after challenge (Figure 5A).

Considering that Tregs function as a regulator for primed T cells, they should serve as suppressors at the challenged site. The above late-phase inhibitory action of Kaede-red Tregs raised the possibility that Tregs migrating from the skin can return to the skin and exert suppressive activity. Kaede/Foxp3$^{hCD2/hCD52}$ mice were sensitized, challenged, and photoconverted as in Figure 3A. Twenty-four hours after photoconversion, the left and right ears were rechallenged with DNFB and vehicle (Figure 5B) or TNCB (Figure 5C), respectively. Another 24 hours later, Kaede-red Tregs were observed in the ears challenged with DNFB, but not in those challenged with vehicle (Figure 5B). The ear rechallenged with a different hapten, TNCB, contained Kaede-red Tregs, but its number was lower than

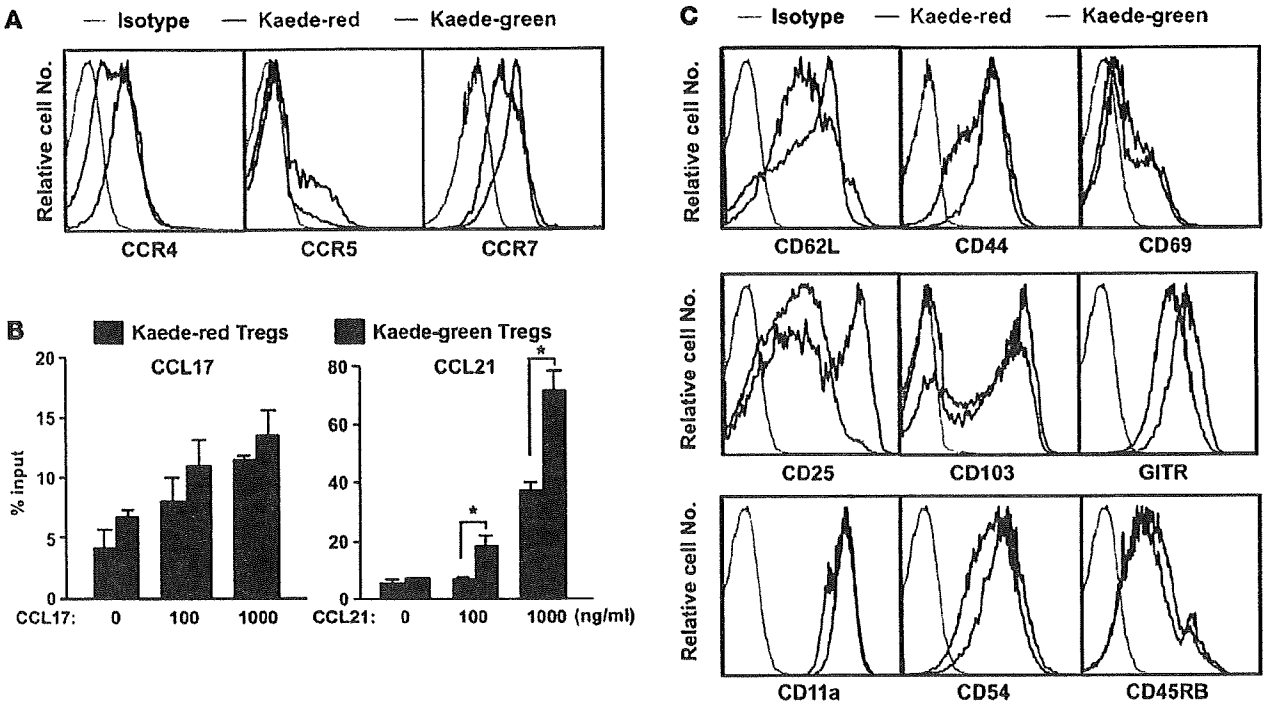

Figure 6

Surface molecule expressions on Kaede-red and Kaede-green cells. (**A**) Chemokine receptor expression. Skin DLN cells were prepared from the mice sensitized, challenged, and photoconverted as in Figure 3A. These LN cells were stained with isotype-matched control, CCR4, CCR5, and CCR7 mAbs, and the expression levels of Kaede-red and Kaede-green Tregs were evaluated by flow cytometry. (**B**) Transwell assay. DLN cells were transferred to the upper chamber of the transwell, and CCL17 or CCL21 was added to the lower chamber. The cells were incubated for 3 hours, and the numbers of Kaede-red and Kaede-green cells that migrated to lower chamber were analyzed by flow cytometry. Data are presented as means ± SD and representative of 2 independent experiments. Student's *t* test was performed between the indicated groups. $^*P < 0.05$. (**C**) Surface molecule expression. LN cells were stained with isotype-matched control, CD62L, CD44, CD69, CD25, and CD103 mAbs, and the expression levels were evaluated by flow cytometry. These data are representative of 3 independent experiments.

that of the ear rechallenged with DNFB (Figure 5C). In addition, Kaede-red Tregs were detected in $CD4^+$ cells of the blood 24 hours after rechallenge (1.79% ± 0.07%, average ± SEM, $n = 3$) (Figure 5D). Moreover, a previous report has suggested that LN cells migrate to the skin (24). We conducted an evaluation of this report by photoconverting DLNs. We sensitized the dorsal skin of mice with DNFB and challenged the abdominal skin with DNFB 4 days later. Two days after challenge, the DLNs of the mice were photoconverted and the ears were rechallenged with DNFB. Twenty-four hours later, the ears of the skin were analyzed by flow cytometric analysis. We found that a substantial fraction of $CD4^+$ $hCD2^-$ non-Tregs and $CD4^+$ $hCD2^+$ Tregs were Kaede-red positive (Supplemental Figure 7). These results suggest that the Tregs that egressed from the skin had a capacity to remigrate to the skin upon challenge.

It has been reported that the representative chemokine receptors essential for migration of lymphocytes into the skin and LNs are CCR4 and CCR7, respectively (9, 14, 25). In addition, CCR5 may be an important chemokine receptor for Tregs to migrate into the skin (26). Kaede-red Tregs expressed higher levels of CCR4 and CCR5 and a lower level of CCR7 than Kaede-green Tregs (Figure 6A). When the skin DLN cells prepared as in Figure 3A were applied to a transwell assay, Kaede-red Tregs showed good chemotactic responses to both CCL17, a ligand for CCR4, and CCL21, a ligand for CCR7, but the chemotaxis of Kaede-red Tregs to CCL21 was weaker than that of Kaede-green Tregs (Figure 6B).

We further analyzed the surface molecules of Kaede-red Tregs in the DLNs of Kaede/Foxp3$^{hCD2/hCD52}$ mice treated as in Figure 3A. Kaede-red Tregs expressed a lower level of CD62L but higher levels of CD44 and CD69 than Kaede-green Tregs (Figure 6C), suggesting that the skin-derived Tregs show a more memory-related T cell phenotype. Interestingly, Kaede-red Tregs contained a $CD25^{hi}$ fraction, which was barely perceptible in Kaede-green Tregs. In addition, Kaede-red Tregs expressed higher levels of CD103, an integrin important for T cell migration into the skin as well as CD11a and CD54, integrins induced upon activation, and a glucocorticoid-induced TNFR family-related gene/protein (GITR), another marker of Tregs (2, 27, 28) (2). However, the expression level of CD45RB was comparable between the Kaede-red and Kaede-green Tregs. These results suggest that Kaede-red Tregs are of the memory/effector phenotype (29) and have a higher potential to migrate to the skin than LN-resident Tregs.

Kinetics and surface phenotype of $CD25^{hi}$ Kaede-red Tregs. The above data (Figure 5A) suggest that Tregs migrating from the skin have a highly potent immunosuppressive capacity even in situ. One of the features of these skin-derived Tregs is the presence of a $CD25^{hi}$ subset (Figure 6C) that has not, to our knowledge, been thoroughly described before. Initially, we sought to characterize the localization of $CD25^{hi}$ Tregs and found that $CD25^{hi}$ cells were substantially detected in Kaede-red Tregs of the DLNs of mice pretreated as in Figure 3A but were only somewhat or marginally detected in

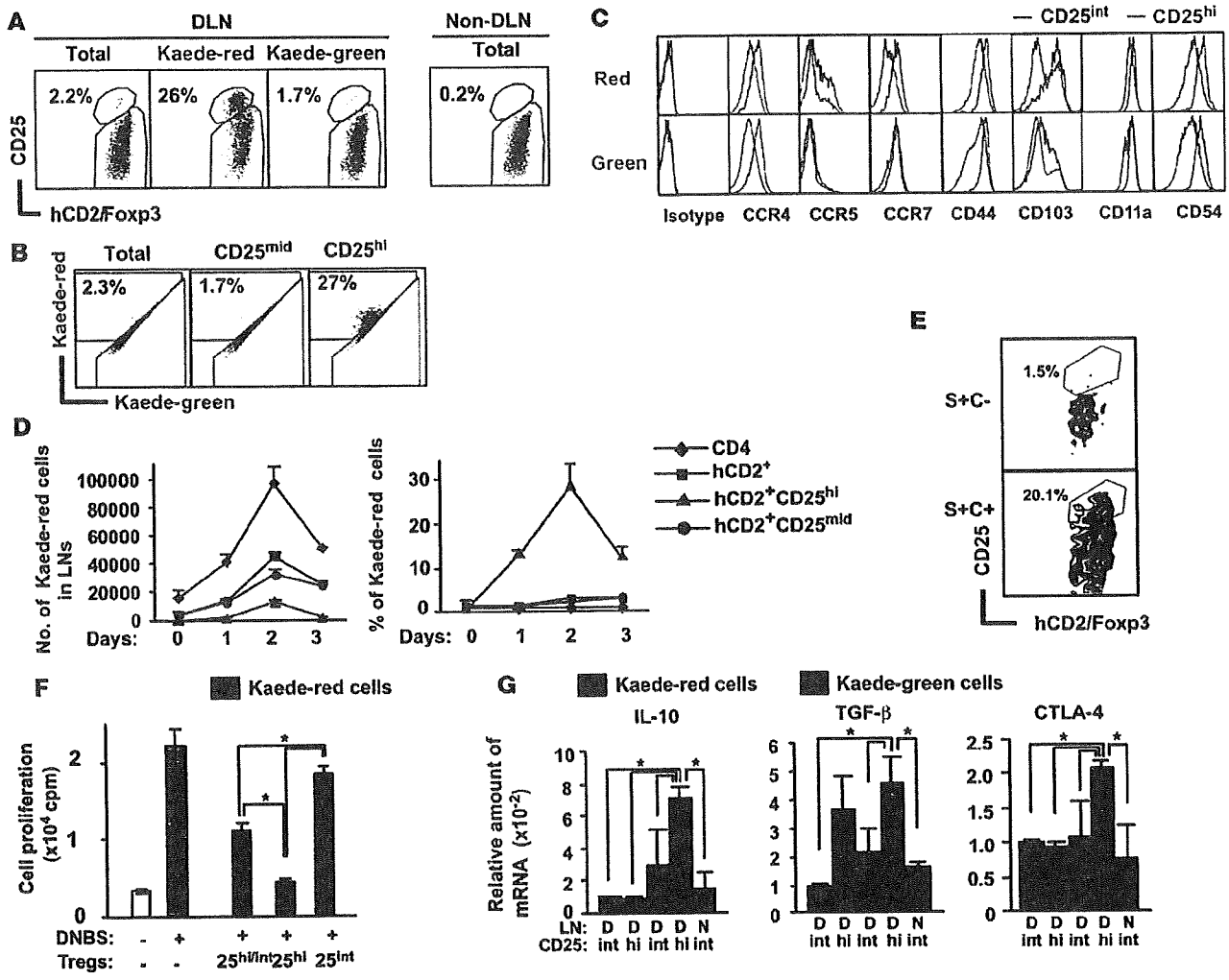

Figure 7

Kinetics and suppression activity of CD25^{hi} Kaede-red migratory Tregs. (**A–C**) Characterization of CD25^{hi} subset. Kaede/Foxp3$^{hCD2/hCD52}$ mice were treated as in Figure 3A, and the expression levels of hCD2/Foxp3 and CD25 on CD4$^+$hCD2/Foxp3$^+$ Tregs in total, Kaede-red, and Kaede-green DLN cells and in non-DLN cells (**A**), the frequency of Kaede-red populations in each population (**B**), and the expression levels of surface markers on Kaede-red or Kaede-green Tregs in the DLNs (**C**) were analyzed. (**D**) Kinetics of T cell migration. Kaede/Foxp3$^{hCD2/hCD52}$ mice were sensitized and challenged as in Figure 3A and photoconverted immediately (day 0), 1 (day 1), 2 (day 2), or 3 (day 3) days after challenge. The number of each subset migrating for 24 hours after photoconversion and the frequency of Kaede-red cells among each subset were measured. (**E**) Foxp3$^{hCD2/hCD52}$ mice were sensitized with DNFB (S+) and challenged with DNFB (C+) or vehicle (C–). Skin suspensions were evaluated for the expression of hCD2/Foxp3 and CD25. (**F**) Skin DLNs cells of sensitized B6 mice were stimulated in the absence or presence of Kaede-red total hCD2$^+$ Tregs (25$^{hi/int}$), CD25^{hi} Tregs (25^{hi}), or CD25^{int} Tregs (25^{int}). (**G**) mRNAs for *Il10* (IL-10), *Tgfb1* (TGF-β), and *Ctla4* (CTLA-4) of Kaede-green CD25^{int} or CD25^{hi} Tregs, Kaede-red CD25^{int} or CD25^{hi} Tregs, or Kaede-green CD25^{int} Tregs in DLNs (D) or non-DLNs (N) were evaluated. The expression level in Kaede-green CD25^{int} Tregs was normalized to 1. Data are presented as means ± SD (n = 3) (**D**, **F**, and **G**). *$P < 0.05$ between indicated groups. (**F** and **G**). Numbers within plots or histograms indicate percentage of cells (**A**, **B**, and **E**).

Kaede-green Tregs of the DLNs or in non-DLNs (Figure 7A). Consistently, the frequency of the Kaede-red population in the CD25^{hi} population was greater than that in the CD25^{mid} population (Figure 7B). These CD25^{hi} Tregs showed higher levels of CCR4, CCR5, CCR7, CD44, CD103, CD11a, and CD54 than CD25^{int} Tregs in the Kaede-red subset (Figure 7C). On the other hand, the expression levels of CCR5 and CD103 of the CD25^{hi} subset in the Kaede-green cells tended to be lower than that in the Kaede-red cells, and the expression of CCR7 in Kaede-green Tregs was similar between CD25^{int} and CD25^{hi} subsets (Figure 7C).

We then examined the kinetics of T cell migration from the skin. Kaede/Foxp3$^{hCD2/hCD52}$ mice were sensitized and challenged as in Figure 3A and photoconverted immediately, 1, 2, or 3 days after challenge. The DLN cells were collected 24 hours after each photoconversion, and the number of Kaede-red CD4$^+$, CD4$^+$hCD2$^+$, CD4$^+$hCD2$^+$CD25^{hi}, and CD4$^+$hCD2$^+$CD25^{mid} cells migrating for 24 hours after photoconversion was determined (Figure 7D). The peak response of cell migration from the skin occurred on day 2 (between 48 and 72 hours after challenge) when the frequency of Tregs among CD4$^+$ T cells migrating from

the skin was high (Figure 7D). In addition, $CD4^+hCD2^+CD25^{hi}$ cells were detected only at this time point (Figure 7D) and showed a high frequency of Kaede-red positivity, especially on day 2 (Figure 7D), suggesting that this subset is replaced by the skin-derived cells more readily than other subsets.

Strong immunosuppressive activity of $CD25^{hi}$ Kaede-red migratory Tregs. To evaluate whether $CD25^{hi}$ Tregs are localized in the skin during immune responses, Kaede/$Foxp3^{hCD2/hCD52}$ mice were sensitized and challenged as in Figure 3A. We detected a significant number of $CD25^{hi}$ Tregs in the challenged local skin, but few in the nonchallenged skin 48 hours after the challenge (Figure 7E), suggesting that $CD4^+hCD2^+CD25^{hi}$ cells are induced in the skin and migrate into the DLNs.

To determine the role of skin-derived $CD25^{hi}$ Tregs, Treg subsets were isolated from the DLNs of mice pretreated as in Figure 3A and cocultured with DLN cells from DNFB-sensitized mice. The $CD25^{hi}$ Tregs showed much stronger suppressive activity on T cell proliferation than the $CD25^{int}$ subset (Figure 7F).

We further examined the mRNA expression profiles of cytokines in the $CD25^{hi}$ Treg subsets. In agreement with the above in vitro result, Kaede-red $CD25^{hi}$ Tregs contained significantly higher amounts of *Il10*, *Tgfb1*, and *Ctla4* than Kaede-red $CD25^{int}$ Tregs in the DLNs, Kaede-green $CD25^{hi}$ or $CD25^{int}$ Tregs in the DLNs, or Kaede-green $CD25^{int}$ Tregs in the non-DLNs, except in the case of *Tgfb1* expression level between Kaede-red $CD25^{hi}$ Tregs and Kaede-green $CD25^{hi}$ Tregs in DLNs (Figure 7G). These results suggest that $CD25^{hi}$ Tregs migrating from the skin play a major suppressive role in cutaneous immune response.

Discussion

In this study, we found that memory/effector phenotype $Foxp3^+$ Tregs as well as $Foxp3^-$ non-Tregs migrated from the skin to DLNs in the steady state. The number of $CD4^+$ T cells in the skin and their migration to DLNs were prominently increased during a cutaneous immune response. Among the migrating T cells, $Foxp3^+$ Tregs constituted one of the major populations. Notably, the Tregs that migrated from the skin returned to the skin upon exposure to an antigen. The migrating Tregs held strong immunosuppressive effect and expressed high levels of mRNA for inhibitory mediators compared with LN-resident Tregs. Moreover, depletion of endogenous Tregs in vivo prolonged the CHS response. Finally, these circulating Tregs specifically included the $CD25^{hi}$ subset that showed an activated phenotype and a very strong inhibitory function on T cell proliferation, with high levels of mRNA for inhibitory mediators. These data suggest that Tregs circulate between blood, skin, and lymphoid tissues to regulate peripheral immune responses.

There have been a few studies that sought to address the possibility of T cell migration from the periphery to LNs. In their experiments, one report suggested that the memory/effector subset of $CD4^+$ T cells is the major constituent in the afferent lymph by cannulation of sheep (6, 11–13), and the other suggested the naive subset is dominant using subcutaneous injection of fluorescent-labeled lymphocytes (14). Recently, effector/memory phenotype of Tregs has been reported to migrate from blood to islet and to DLNs sequentially using an islet allograft model with transfer of in vitro-induced Tregs (30). However, since all the above experiments require traumatic or artificial procedures to label T cells in the periphery, it remains unknown whether endogenous T cells egress from the periphery into DLNs under pathophysiological conditions. In this study, using the Kaede-Tg system, we have clearly demonstrated that a subset of T cells with memory/effector phenotype migrates to DLNs in the steady state and during a cutaneous immune response. During the immune response, Tregs are the major constituents and they return to the skin upon exposure to an antigen. Therefore, as naive T cells circulate between blood and LNs, cells of the memory/effector T cell phenotype, especially Tregs, seem to circulate between blood and the skin. In this study, we used the skin as a representative of the peripheral tissues, but it would be of interest to explore this issue in other peripheral tissues, such as lungs and intestines.

To date, the roles of externally transferred Tregs in CHS have been reported (31); however, the regulatory activity of endogenous Tregs has not been fully assessed. In this study, we found that depletion of Tregs during the elicitation phase prolonged the CHS response. In addition, CHS-induced migratory Tregs suppressed the proliferation of DNFB-sensitized LN cells in a ratio as low as 1:100 (Tregs to LN cells), but such an inhibitory effect was not observed in non-antigen-specific mitogen-induced T cell proliferation systems. Therefore, Tregs circulating between the skin and LNs may inhibit not only T cells, but also antigen-presenting cells, such as dendritic cells, or antigen-presenting cell–T cell interactions. Moreover, subcutaneous injection of migratory Tregs into the skin suppressed CHS more markedly than that of LN-resident Tregs. Similar findings were observed when these Tregs were transferred intravenously (data not shown), suggesting that Tregs migrating from the skin hold a high immunosuppressive potential.

The $CD25^{hi}$ subset that migrated from the skin seems to have an activated phenotype, indicated by the positivity of CD25 and CD103. It has been reported that transfer of preactivated $CD25^+CD103^+$ cells strongly suppressed T cell proliferation (32) and $CD25^+CD103^-$ cells are the main producer of IL-10 after TCR stimulation (29). The $CD25^{hi}$ subset in our finding expresses high levels of CD103 and IL-10 and strong suppressive capacity and phenotype, consistent with an activated effector/memory Treg subset (28, 33). It should be noted that we demonstrate that the $CD25^{hi}$ subset was localized in the skin and only transiently migrated from the skin after CHS elicitation. Thus, the role of skin in generation, education, and spatiotemporal regulation of this $CD25^{hi}$ subset during immune responses needs to be elucidated in the future, which may lead us to understand the role of peripheral tissues in regulation of immune responses.

Notably, Treg cell circulation was remarkably induced during cutaneous immune responses. Therefore, we have focused on the roles of Tregs instead of effector/memory T cells migrating from the skin. In fact, the administration of migratory Tregs strongly suppressed CHS response at the later phase after a challenge (Figure 5A), and in vivo depletion of Tregs prolonged the CHS response, particularly during the later phase (Figure 4B). These results suggest that these circulating Tregs might be involved in the termination of immune responses. However, immune responses and homeostasis are regulated and maintained by the balance between Tregs and effector/memory T cells, and it has been thought that CHS occurs by the dominance of effector/memory T cells over Tregs. Hence, it is intriguing that the elicitation of CHS induces Tregs despite their possible antagonistic role for the development of acquired immune response. In this sense, it will be of interest to explore more the roles of effector/memory T cells and Tregs migrating from the skin in regulating immune response. Clarification of these issues will lead not only to understanding of the novel mechanism of cutaneous immune responses but also to control of systemic immune responses through modulating cutaneous immunity.

Methods

Mice and photoconversion. Tg mice carrying Kaede cDNA under the CAG promoter were established previously (17). These mice with B6 genetic background expressed photoconvertible Kaede in all of their cell types. It should be nored that the use of violet light (436 nm) rather than harmful UVA (320–400 nm) or UVB (290–320 nm) allowed us to photoconvert Kaede in the cells with no detectable damage (17).

Because of the moiety of its wavelength, violet light exposure penetrates through the skin to subcutaneous tissue, but not further (data not shown). Although the exposure of Kaede to violet light permanently changes its structure and photoconverted Kaede has a very long biological half-life in lymphocytes, cell proliferation dilutes photoconverted Kaede with newly synthesized nonphotoconverted Kaede, and after several cell divisions, the detection of red fluorescence becomes difficult (17). Moreover, exposure of the cells to violet light for 10 minutes has no effect on T and B cell proliferation (17). To exclude the immunomodulatory effect of photoconversion in vivo, we used the CHS model. Photoconversion of the abdominal skin immediately after sensitization on the abdomen did not affect CHS response (data not shown). When mRNA levels of *Il1b* were examined 6 hours after photoconversion (436 nm) or low-dose (3 kJ/m^2) UVB exposure, a significant increase of mRNA levels of *Il1b* was observed by UVB but not by photoconversion (Supplemental Figure 8). Therefore, we assume that photoconversion of the skin does not provoke significant inflammation in the skin or inflammatory stimuli in keratinocytes.

B6 Foxp3$^{hCD2/hCD52}$ mice were generated by homologous recombination in a B6-derived ES cell line using a targeting construct in which cDNA encoding a human CD2 and human CD52 fusion protein along with an intraribosomal entry site was inserted into the 3′ untranslated region of the endogenous Foxp3 locus (18). All CD4$^+$Foxp3$^+$ cells expressed hCD2, but CD4$^+$ Foxp3$^-$ cells did not (data not shown), indicating that the expression of the human CD2 reporter faithfully reflects the intracellular expression of Foxp3 in Foxp3$^{hCD2/hCD52}$ mice. Foxp3$^{hCD2/hCD52}$ mice (18) were intercrossed with Kaede-Tg mice to generate Kaede/Foxp3$^{hCD2/hCD52}$ mice for further evaluation. These mice were bred in specific pathogen-free facilities at Kyoto University or RIKEN. All experimental procedures were approved by the Institutional Animal Care and Use Committee of Kyoto University Faculty of Medicine and RIKEN.

Antibodies and flow cytometry. Fluorochrome-conjugated or biotinylated anti-human CD2, anti-mouse CD4, CD11a, CD11c, CD25, CD44, CD45RB, CD62L, CD69, CD103, GITR, CCR4, CCR5, and CCR7 mAbs were obtained from BD Biosciences, eBioscience, or Biolegend. Data were acquired using the JSAN system (Bay bioscience) or FACSCanto II flow cytometry system (BD Biosciences) and analyzed with FlowJo (TreeStar).

Cell preparation from the skin and cell sorting. Briefly, the ears were removed and split into dorsal and ventral halves, and cartilage was removed. The skin of the ears was floated on 0.25% trypsin/EDTA for 30 minutes at 37°C. Then the epidermis was peeled from the dermis, and both epidermis and dermis were minced with forceps. The minced tissues were incubated for 1 hours in collagenase II (Worthington Biochemical) containing hyaluronidase and DNaseI (Sigma-Aldrich). The cell suspensions were filtered with 40 μm of cell strainer.

For cell sorting, Kaede-red Tregs or Kaede-green Tregs were purified from inguinal and axillary LNs of Kaede/Foxp3$^{hCD2/hCD52}$ mice. Briefly, the mice were sensitized and challenged with DNFB in the same way as the B6 mice for DNBS-induced cell proliferation. Two days after the challenge, cells of abdominal skin were photoconverted, and single-cell suspensions were prepared from inguinal and axillary LNs 24 hours after photoconversion. The cells of each population were sorted by the FACSAria II flow cytometry system (BD Bioscience).

Photoconversion, CHS model, in vivo Treg depletion, and cell proliferation assay. Photoconversion of the skin was performed as described previously (17). Briefly, mice were anesthetized, shaved, and exposed to violet light at 95 mW/cm^2 with a 436-nm bandpass filter using Spot UV curing equipment (SP500; USHIO).

For the CHS model, mice were immunized by application of 25 μl of 0.5% DNFB (Nacalai Tesque) in 4:1 (wt/vol) acetone/olive oil to their shaved abdomens on day 0 and challenged on the right ear on day 5 with 20 μl of 0.3% (wt/vol) DNFB (34). Ear thickness was measured before and after challenge, and ear-thickness change was calculated.

For Treg depletion in vivo, mice were injected with Campath-1G Ab through the tail vein (0.5 mg/body) 1 day before the CHS challenge (22). The injection was repeated every 4 days throughout the experiment. The same amount of vehicle or rat IgG (0.5 mg/body; Sigma-Aldrich) was used as a control.

For DNBS- or TNBS-dependent cell proliferation, mice were sensitized with 50 μl of 0.5% DNFB (wt/vol) or 50 μl of 5% TNCB (Tokyo Kasei) (wt/vol) in acetone/olive oil (4/1; vol/vol) on the dorsal skin, and 5 days later, single-cell suspensions were prepared from inguinal and axillary LNs. CD25-positive cells were depleted from the cells by Auto-MACS (Miltenyi Biotec) using PE-labeled anti-mouse CD25 antibody (eBioscience) and magnetic microbeads coated with anti-PE (Miltenyi Biotec). Less than 1% of Foxp3$^+$ cells were present in the remaining LN cells. 7×10^5 LN cells/well in a 96-well plate were cultured in RPMI 1640 containing 10% FBS with or without 50 μg/ml DNBS (Alfa Aesar) for 3 days. For TNBS stimulation, the LN cells were incubated in 2.5 mM TNBS (Tokyo Kasei) in PBS for 20 minutes at 37°C and subsequently washed 3 times in PBS, and 7×10^5 cells/well in a 96-well plate were cultured in RPMI 1640 containing 10% FBS for 3 days. Cells were pulsed with 0.5 μCi ^{3}H-thymidine for the last 24 hours of culture and subjected to liquid scintillation counting.

For the proliferation assay of anti-CD3 stimulation, spleen CD4$^+$ cells deprived of CD25$^+$ cells were sorted by auto-MACS. Then, 5×10^4 cells/well were cultured in a 96-well plate coated with 1 μg/ml of anti-CD3 antibody for 72 hours. For the last 24 hours, cells were pulsed with 0.5 μCi ^{3}H-thymidine, and its incorporation was measured.

Quantitative RT-PCR analysis. Total RNA from purified cells was isolated with the RNeasy Mini Kit (QIAGEN). Quantitative RT-PCR with the Light Cycler real-time PCR apparatus was performed according to the instructions of the manufacturer (Roche) by monitoring the synthesis of double-stranded DNA during the various PCR cycles using SYBR Green I (Roche). For each sample, duplicate test reactions were analyzed for expression of the gene of interest, and results were normalized to those of the *Gapdh* mRNA.

In vivo immunosuppression assay. A total of 4×10^3 cells of isolated Kaede-red Tregs or Kaede-green Tregs in 20 μl PBS were subcutaneously injected into the ventral surface of each ear. Ear thickness was measured for each mouse before and at the indicated time point after elicitation with a micrometer, and the difference was expressed as ear swelling (n = 4–6 in each group).

Chemotaxis assay. Skin cell suspensions of Foxp3$^{hCD2/hCD52}$ mice were tested for transmigration across uncoated 5-μm transwell filters (Corning Costar Corp.) for 3 hours to CCL21 (R&D Systems) or medium in the lower chamber, and the numbers of cells that migrated to the lower chamber were determined by flow cytometry (35). The migration index was shown as a percentage of input by dividing with total input cells in upper chamber.

Statistics. Data were analyzed with the unpaired Student's 2-tailed t test unless otherwise stated. A P value of less than 0.05 was considered to be significant.

Acknowledgments

This study was supported in part by grants from the Ministry of Education, Culture, Sports, Science, and Technology of Japan and the Ministry of Health, Labor, and Welfare of Japan.

Received for publication August 24, 2009, and accepted in revised form December 16, 2009.

Address correspondence to: Kenji Kabashima, Department of Dermatology and Center for Innovation in Immunoregulative Technology and Therapeutics, Kyoto University, Yoshida-Konoe, Kyoto, 606-8501, Japan. Phone: 81.75.753.9502; Fax: 81.75.753.9500; E-mail: kaba@kuhp.kyoto-u.ac.jp. Or to: Michio Tomura, Laboratory for Autoimmune Regulation, Research Center for Allergy and Immunology, RIKEN, 1-7-22 Suehiro-cho, Tsurumi, Yokohama City, Kanagawa 230-0045, Japan. Phone: 81.45.503.9699; Fax: 81.45.503.9697; E-mail: tomura@rcai.riken.jp.

1. Korn T, Bettelli E, Oukka M, Kuchroo VK. IL-17 and Th17 cells. *Annu Rev Immunol.* 2009;27:485–517.
2. Sakaguchi S, Yamaguchi T, Nomura T, Ono M. Regulatory T cells and immune tolerance. *Cell.* 2008;133(5):775–787.
3. Lu LF, Rudensky A. Molecular orchestration of differentiation and function of regulatory T cells. *Genes Dev.* 2009;23(11):1270–1282.
4. Gowans JL, Knight EJ. The route of re-circulation of lymphocytes in the rat. *Proc R Soc Lond B Biol Sci.* 1964;159:257–282.
5. Gowans JL. The recirculation of lymphocytes from blood to lymph in the rat. *J Physiol.* 1959; 146(1):54–69.
6. Mackay CR, Marston WL, Dudler L. Naive and memory T cells show distinct pathways of lymphocyte recirculation. *J Exp Med.* 1990;171(3):801–817.
7. Matloubian M, et al. Lymphocyte egress from thymus and peripheral lymphoid organs is dependent on S1P receptor 1. *Nature.* 2004;427(6972):355–360.
8. Campbell DJ, Debes GF, Johnston B, Wilson E, Butcher EC. Targeting T cell responses by selective chemokine receptor expression. *Semin Immunol.* 2003;15(5):277–286.
9. Campbell JJ, et al. The chemokine receptor CCR4 in vascular recognition by cutaneous but not intestinal memory T cells. *Nature.* 1999;400(6746):776–780.
10. Homey B, et al. CCL27-CCR10 interactions regulate T cell-mediated skin inflammation. *Nat Med.* 2002;8(2):157–165.
11. Olszewski WL, Grzelak I, Ziolkowska A, Engeset A. Immune cell traffic from blood through the normal human skin to lymphatics. *Clin Dermatol.* 1995;13(5):473–483.
12. Olszewski WL. The lymphatic system in body homeostasis: physiological conditions. *Lymphat Res Biol.* 2003;1(1):11–21; discussion 21–24.
13. Mackay CR, Kimpton WG, Brandon MR, Cahill RN. Lymphocyte subsets show marked differences in their distribution between blood and the afferent and efferent lymph of peripheral lymph nodes. *J Exp Med.* 1988;167(6):1755–1765.
14. Debes GF, et al. Chemokine receptor CCR7 required for T lymphocyte exit from peripheral tissues. *Nat Immunol.* 2005;6(9):889–894.
15. Ando R, Hama H, Yamamoto-Hino M, Mizuno H, Miyawaki A. An optical marker based on the UV-induced green-to-red photoconversion of a fluorescent protein. *Proc Natl Acad Sci U S A.* 2002;99(20):12651–12656.
16. Mizuno H, et al. Photo-induced peptide cleavage in the green-to-red conversion of a fluorescent protein. *Mol Cell.* 2003;12(4):1051–1058.
17. Tomura M, et al. Monitoring cellular movement in vivo with photoconvertible fluorescence protein "Kaede" transgenic mice. *Proc Natl Acad Sci U S A.* 2008;105(31):10871–10876.
18. Komatsu N, et al. Heterogeneity of natural Foxp3+ T cells: a committed regulatory T-cell lineage and an uncommitted minor population retaining plasticity. *Proc Natl Acad Sci U S A.* 2009;106(6):1903–1908.
19. Fontenot JD, Rasmussen JP, Gavin MA, Rudensky AY. A function for interleukin 2 in Foxp3-expressing regulatory T cells. *Nat Immunol.* 2005; 6(11):1142–1151.
20. Randolph GJ, Ochando J, Partida-Sanchez S. Migration of dendritic cell subsets and their precursors. *Annu Rev Immunol.* 2008;26:293–316.
21. Hirahara K, et al. The majority of human peripheral blood CD4+CD25highFoxp3+ regulatory T cells bear functional skin-homing receptors. *J Immunol.* 2006;177(7):4488–4494.
22. Hale G, Cobbold SP, Waldmann H, Easter G, Matejtschuk P, Coombs RR. Isolation of low-frequency class-switch variants from rat hybrid myelomas. *J Immunol Methods.* 1987;103(1):59–67.
23. Wing K, Onishi Y, et al. CTLA-4 control over Foxp3+ regulatory T cell function. *Science.* 2008;322(5899):271–275.
24. Reiss Y, Proudfoot AE, Power CA, Campbell JJ, Butcher EC. CC chemokine receptor (CCR)4 and the CCR10 ligand cutaneous T cell-attracting chemokine (CTACK) in lymphocyte trafficking to inflamed skin. *J Exp Med.* 2001;194(10):1541–1547.
25. Randolph GJ, Ochando J, Partida SNS. Migration of dendritic cell subsets and their precursors. *Annu Rev Immunol.* 2007;26:293–316.
26. Yurchenko E, et al. CCR5-dependent homing of naturally occurring CD4+ regulatory T cells to sites of Leishmania major infection favors pathogen persistence. *J Exp Med.* 2006;203(11):2451–2460.
27. Baekkevold ES, et al. A role for CCR4 in development of mature circulating cutaneous T helper memory cell populations. *J Exp Med.* 2005;201(7):1045–1051.
28. Huehn J, et al. Developmental stage, phenotype, and migration distinguish naive- and effector/memory-like CD4+ regulatory T cells. *J Exp Med.* 2004;199(3):303–313.
29. Banz A, et al. A unique subpopulation of CD4+ regulatory T cells controls wasting disease, IL-10 secretion and T cell homeostasis. *Eur J Immunol.* 2003;33(9):2419–2428.
30. Zhang N, et al. Regulatory T cells sequentially migrate from inflamed tissues to draining lymph nodes to suppress the alloimmune response. *Immunity.* 2009;30(3):458–469.
31. Ring S, Oliver SJ, Cronstein BN, Enk AH, Mahnke K. CD4+CD25+ regulatory T cells suppress contact hypersensitivity reactions through a CD39, adenosine-dependent mechanism. *J Allergy Clin Immunol.* 2009;123(6):1287–1296 e1282.
32. Siegmund K, et al. Migration matters: regulatory T-cell compartmentalization determines suppressive activity in vivo. *Blood.* 2005;106(9):3097–3104.
33. Miyara M, et al. Functional delineation and differentiation dynamics of human CD4+ T cells expressing the FoxP3 transcription factor. *Immunity.* 2009;30(6):899–911.
34. Kabashima K, Arima Y, Miyachi Y. Contact dermatitis from lacquer in a 'Go' player. *Contact Dermatitis.* 2003;49(6):306–307.
35. Kabashima K, et al. Thromboxane A2 modulates interaction of dendritic cells and T cells and regulates acquired immunity. *Nat Immunol.* 2003;4(7):694–701.

Compensatory role of Langerhans cells and langerin-positive dermal dendritic cells in the sensitization phase of murine contact hypersensitivity

To the Editor:

In the initiation of skin immune responses, cutaneous dendritic cells (DCs) play a central role by presenting antigen to naive T cells and supporting T-cell expansion and polarization. Formerly, it was generally believed that 2 types of DCs existed in the skin, epidermal langerin-positive ($CD207^+$) Langerhans cells (LCs) and dermal DCs (dDCs). Recently, it has been revealed that dDCs are divided into 2 populations according to their expression of langerin: langerin-positive dDCs and langerin-negative dDCs.[1-3] LCs have long been regarded as essential cells for the establishment of sensitization in patients with contact hypersensitivity (CHS), but this concept is now being challenged by recent analyses using LC ablation murine models.[3-5] In this study we have revealed that LCs and langerin-positive dDCs play a compensatory role in the sensitization phase of murine CHS.

At present, there are 2 types of LC ablation murine models. The first uses mice that express enhanced green fluorescent protein (eGFP) fused with a diphtheria toxin (DT) receptor (DTR) under the control of the langerin promoter, which are known as langerin-eGFP-DTR mice,[3,4] and langerin-DTR mice.[6-8] In these knock-in mice, both LCs and langerin-positive dDCs are detected based on their eGFP expression, and both are completely depleted by administration of DT. Once depleted, LCs do not repopulate for at least 4 weeks, whereas the number of langerin-positive dDCs in the skin recovers to the basal level about 14 days after depletion by DT.[3-5] Using these mice, some studies have reported that depletion of LCs alone in the sensitization phase leads to an insufficient CHS response, suggesting the importance of LCs in sensitization, especially to low doses of hapten.[6,7] Other studies have reported that depletion of LCs alone does not impair CHS; rather, only depletion of both LCs and langerin-positive dDCs attenuates CHS, suggesting that LCs are not necessarily essential for sensitization and that langerin-positive dDCs are rather important mediators for sensitization in CHS response.[3,4] The second LC ablation model uses transgenic langerin-DTA mice, which constitutively lack LCs.[5] These LC-deficient mice exhibit enhanced CHS responses, suggesting that LCs play a regulatory role rather than a stimulating role. Therefore the role of LCs in sensitization is still controversial and has not yet been fully elucidated. Furthermore, the necessity of langerin-positive dDCs in the sensitization phase of CHS remains unknown.

In this study we sought to characterize the respective roles of LCs and langerin-positive dDCs in the sensitization phase of CHS. To this end, we have established an experimental system in which we sensitized mice under 3 different depletion conditions: in the absence of both LCs and langerin-positive dDCs, in the absence of LCs alone, and in the absence of langerin-positive dDCs alone. First, we generated mice lacking only langerin-positive dDCs using a bone marrow transplantation (BMT) system. LCs are radioresistant, and LCs of host origin persist in the epidermis of the recipient for at least 1 year after BMT.[9] In addition, although a population of radioresistant dDCs has been reported,[10] langerin-positive dDCs are radiosensitive and are reconstituted with donor-derived cells after BMT.[2] Accordingly, we irradiated 6-week-old congenic $CD45.1^+$ $CD45.2^+$ C57BL/6 mice with 9 Gy and transferred 2×10^6 bone marrow cells from $CD45.1^-$ $CD45.2^+$ langerin-eGFP-DTR mice[4] into the irradiated mice. After 2 months, more than 95% of the blood cells in the recipient mice had been reconstituted with CD45.2 single-positive cells.

To confirm reconstitution, the epidermis and dermis of bone marrow chimeric (BMC) mice and langerin-eGFP-DTR mice were separated through treatment with trypsin/EDTA (Sigma-Aldrich, St Louis, Mo), and single-cell suspensions of epidermis and dermis were prepared through treatment with collagenase type 2 (Worthington, Lakewood, NJ) for 1 hour. These single-cell suspensions were stained with fluorescent-labeled antibodies (all from eBioscience, San Diego, Calif) and analyzed by using the FACSCanto II flow cytometric system (BD Bioscience, San

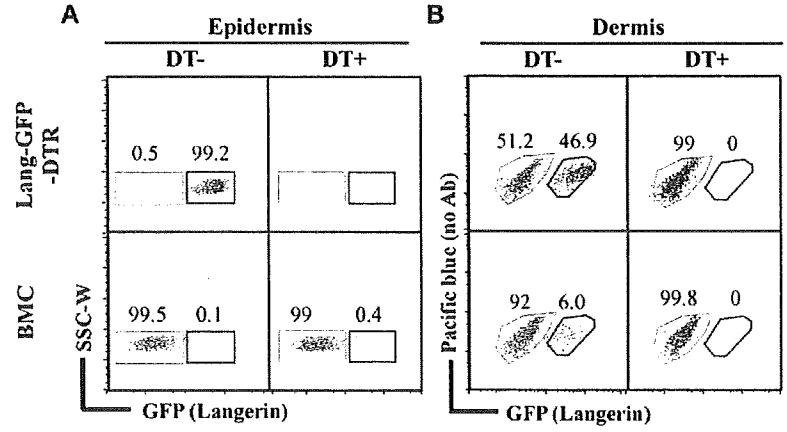

FIG 1. Effect of DT on GFP^+ cells. The $CD11c^+$ MHC class II^+ cells of the epidermis and dermis from either langerin-eGFP-DTR *(Lang-GFP-DTR)* mice *(upper panels)* or BMC mice *(lower panels)* were analyzed by means of flow cytometry for the expression of GFP. The frequency of GFP^+ and GFP cells in the epidermis **(A)** and dermis **(B)** before *(DT−; left panels)* and after *(DT+; right panels)* are shown.

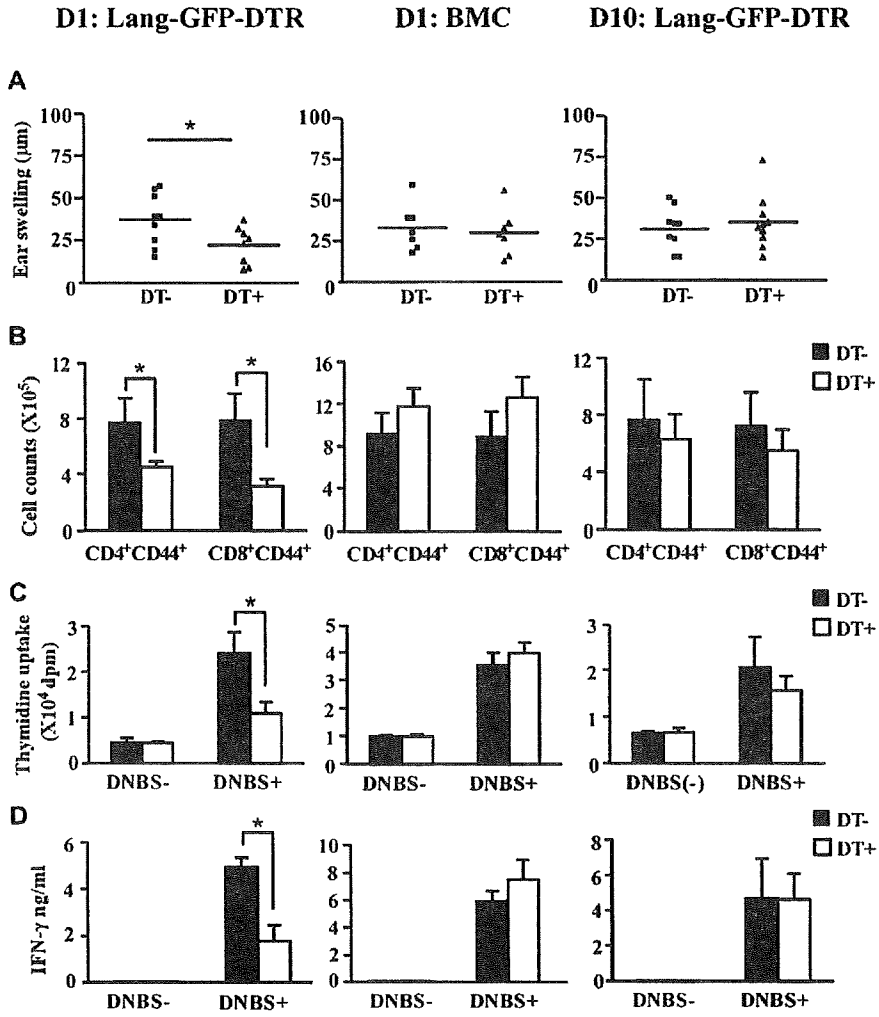

FIG 2. Role of LCs and langerin-positive dDCs in the sensitization phase of CHS. **A**, CHS response. **B**, The number of $CD44^+$ T cells in draining lymph nodes 6 days after sensitization. **C**, DNBS-induced cell proliferation. LN cells (1×10^6) were cultured with or without DNBS stimulation in a 96-well plate for 72 hours; tritiated thymidine was added for the last 12 hours. **D**, IFN-γ level. The levels of IFN-γ in the culture medium 72 hours after incubation were measured with an ELISA kit. Data are presented as means ± SDs and are representative of 3 experiments with similar results. $*P < .05$.

Diego, Calif) and FlowJo software (Tree Star, Ashland, Ore; Fig 1). As reported previously, in langerin-eGFP-DTR mice almost all MHC class II^+ $CD11c^+$ DCs in the epidermis were langerin positive (LCs; Fig 1, *A*, upper left), and about half of MHC class II^+ $CD11c^+$ DCs in the dermis were langerin positive (migrating LCs and langerin-positive dDCs; Fig 1, *B*, upper left). Both langerin-positive subsets in the epidermis and dermis were depleted by intraperitoneal administration of 1 μg of DT (Sigma-Aldrich) into each mouse (Fig 1, *A* and *B*, upper right panels). All MHC class II^+ $CD11c^+$ LCs in the epidermis of BMC mice were eGFP negative (Fig 1, *A*, lower left), suggesting that LCs were not reconstituted by the donor cells. Furthermore, this LC subset was not depleted by treatment with DT (Fig 1, *A*, lower panels). On the other hand, an eGFP-positive subset was detected in MHC class II^+ $CD11c^+$ DCs in the dermis (langerin-positive dDCs; Fig 1, *B*, lower left); this subset completely disappeared 1 day after administration of DT (Fig 1, *B*, lower right). To further confirm the reconstitution of langerin-positive dDCs, we evaluated the expression of eGFP in dermal MHC class II^+ $CD11c^+$ $EpCAM^-$ $CD103^+$ langerin-positive DCs and confirmed that more than 95% of them were eGFP positive (see Fig E1 in this article's Online Repository at www.jacionline.org), which suggests that langerin-positive dDCs were reconstituted quite well with langerin-eGFP-DTR bone marrow cells. In addition, this subset was almost completely depleted by administration of DT (see Fig E2 in this article's Online Repository at www.jacionline.org). These results indicate that only langerin-positive dDCs are reconstituted as a result of irradiation and depleted by DT administration.

Using these BMC mice, we investigated the role of langerin-positive dDCs in the sensitization phase of CHS. We used langerin-eGFP-DTR mice to evaluate the effect of depletion of both LCs and langerin-positive dDCs. Because it has been reported that CHS response was impaired in DT-treated langerin-eGFP-DTR mice sensitized with low-dose dinitrofluorobenzene (DNFB),[3] we followed the same protocol: we sensitized

mice with 25 μL of 0.3% (wt/vol) DNFB (Nacalai Tesque, Kyoto, Japan) in acetone/olive oil (4:1) on shaved abdominal skin and challenged the mice with 20 μL of 0.15% DNFB in acetone/olive oil (4:1) on ear skin 5 days later. The ear-thickness change was measured at 1 mm medial from the periphery of the ear 24 hours after the challenge with a thickness gauge (Teclock PG-20, Nagano, Japan). As in previous reports,[3] the CHS response was reduced in langerin-eGFP-DTR mice that had been treated with DT 1 day before sensitization (Fig 2, *A*). In addition to measuring ear-swelling response, which is affected not only by the intensity of the immune response but also by nonimmunologic factors, such as vascular leakage and keratinocyte irritability, we also assessed the induction of $CD44^+$ memory T cells in draining lymph nodes, as well as antigen-specific T-cell clones and their differentiation into T_H1 cells. The numbers of $CD4^+$ $CD44^+$ and $CD8^+$ $CD44^+$ memory T cells in draining lymph nodes 6 days after sensitization were significantly reduced in DT-treated langerin-eGFP-DTR mice (Fig 2, *B*, left). *In vitro* antigen-specific cell proliferation and the amount of IFN-γ in the supernatant were also significantly reduced in the DT-treated group (Fig 2, *C* and *D*, left panels). As a control, wild-type C57BL/6 mice were also treated with DT, but DT treatment did not affect these parameters (data not shown). These results indicate that simultaneous depletion of LCs and langerin-positive dDCs impairs sensitization with low-dose DNFB.

We next applied this CHS protocol to BMC mice, either untreated or treated with DT 1 day before sensitization, and examined the same parameters. All parameters were comparable between vehicle-treated mice and DT-treated mice (Fig 2, middle panels), indicating that langerin-positive dDCs are not essential in the sensitization phase of CHS.

We also used this CHS protocol to examine the involvement of LCs. We treated langerin-eGFP-DTR mice with DT 10 days before sensitization and examined the same parameters in the same way. All the parameters were equivalent between the vehicle-treated group and the DT-treated group (Fig 2, right panels), indicating that LCs alone are not essential in the sensitization phase of CHS.

It has been reported that treatment with DT results in impairment of the CHS response in langerin-eGFP-DTR mice when the mice are sensitized with low doses of DNFB[3] but not when they are sensitized with standard doses of DNFB.[4] Therefore we followed the standard CHS protocol, namely sensitization with 25 μL of 0.5% DNFB on the abdominal skin and elicitation with 20 μL of 0.3% DNFB on the ear skin. We administered vehicle or DT to langerin-eGFP-DTR mice 1 day before sensitization and examined the parameters discussed above. All parameters were comparable between vehicle-treated mice and DT-treated mice (CHS, 122.2 ± 16.2 μm [vehicle] vs 114.7 ± 14.6 μm [DT], n = 6; cell proliferation, 31,564 ± 2,955 cpm [vehicle] vs 33,661 ± 3,364 cpm [DT], n = 3; and IFN-γ production, 14,210 ± 3,370 pg/mL [vehicle] vs 18,720 ± 3,560 pg/mL [DT], n = 3), suggesting that neither langerin-positive DCs nor LCs are essential in sensitization when standard DNFB concentrations are used.

Although langerin-positive dDCs are currently receiving attention as mediators of sensitization, our results suggest that antigen presentation by langerin-positive dDCs is not necessarily the main pathway involved in sensitization.

In conclusion, our results suggest that neither langerin-positive dDCs alone nor LCs alone are essential in sensitization; rather, both types play compensatory roles in the sensitization phase of CHS in a low-dose DNFB sensitization protocol, although not in a standard-dose DNFB sensitization protocol. Differences in antigens (eg, oxazolone in Bennett et al[7] and DNFB in Bursch et al[3]), antigen concentrations, and depletion timing might explain the phenotypic differences among the LC ablation models.[3-7] Further detailed analysis under different conditions is needed to reveal the functions and significance of LCs and langerin-positive dDCs in CHS.

Tetsuya Honda, MD, PhD[a]
Saeko Nakajima, MD[a]
Gyohei Egawa, MD[a,b]
Kouetsu Ogasawara, PhD[c]
Bernard Malissen, MD, PhD[d]
Yoshiki Miyachi, MD, PhD[a]
Kenji Kabashima, MD, PhD[a,b]

From [a]the Department of Dermatology and [b]the Center for Innovation in Immunoregulative Technology and Therapeutics, Kyoto University Graduate School of Medicine, Kyoto, Japan; [c]the Department of Immunobiology, Institute of Development, Aging and Cancer, Tohoku University Sendai, Japan; and [d]Centre d'Immunologie de Marseille-Luminy, Université de la Méditerrannée, Marseille, France. E-mail: hontetsu@kuhp.kyoto-u.ac.jp; kaba@kuhp.kyoto-u.ac.jp.

Supported in part by grants-in-aid for scientific research from the Japanese Ministry of Education, Culture, Sports, Science and Technology; the National Institute of Biomedical Innovation of Japan; and Shiseido Research Foundation.

Disclosure of potential conflict of interest: The authors have declared that they have no conflict of interest.

REFERENCES

1. Poulin LF, Henri S, de Bovis B, Devilard E, Kissenpfennig A, Malissen B. The dermis contains langerin+ dendritic cells that develop and function independently of epidermal Langerhans cells. J Exp Med 2007;204:3119-31.
2. Ginhoux F, Collin MP, Bogunovic M, Abel M, Leboeuf M, Helft J, et al. Blood-derived dermal langerin+ dendritic cells survey the skin in the steady state. J Exp Med 2007;204:3133-46.
3. Bursch LS, Wang L, Igyarto B, Kissenpfennig A, Malissen B, Kaplan DH, et al. Identification of a novel population of Langerin+ dendritic cells. J Exp Med 2007;204:3147-56.
4. Kissenpfennig A, Henri S, Dubois B, Laplace-Builhe C, Perrin P, Romani N, et al. Dynamics and function of Langerhans cells in vivo: dermal dendritic cells colonize lymph node areas distinct from slower migrating Langerhans cells. Immunity 2005;22:643-54.
5. Kaplan DH, Jenison MC, Saeland S, Shlomchik WD, Shlomchik MJ. Epidermal Langerhans cell-deficient mice develop enhanced contact hypersensitivity. Immunity 2005;23:611-20.
6. Bennett CL, van Rijn E, Jung S, Inaba K, Steinman RM, Kapsenberg ML, et al. Inducible ablation of mouse Langerhans cells diminishes but fails to abrogate contact hypersensitivity. J Cell Biol 2005;169:569-76.
7. Bennett CL, Noordegraaf M, Martina CA, Clausen BE. Langerhans cells are required for efficient presentation of topically applied hapten to T cells. J Immunol 2007;179:6830-5.
8. Nagao K, Ginhoux F, Leitner WW, Motegi S, Bennett CL, Clausen BE, et al. Murine epidermal Langerhans cells and langerin-expressing dermal dendritic cells are unrelated and exhibit distinct functions. Proc Natl Acad Sci U S A 2009;106:3312-7.
9. Merad M, Hoffmann P, Ranheim E, Slaymaker S, Manz MG, Lira SA, et al. Depletion of host Langerhans cells before transplantation of donor alloreactive T cells prevents skin graft-versus-host disease. Nat Med 2004;10:510-7.
10. Bogunovic M, Ginhoux F, Wagers A, Loubeau M, Isola LM, Lubrano L, et al. Identification of a radio-resistant and cycling dermal dendritic cell population in mice and men. J Exp Med 2006;203:2627-38.

doi:10.1016/j.jaci.2009.12.005

J ALLERGY CLIN IMMUNOL
□□□ 2010

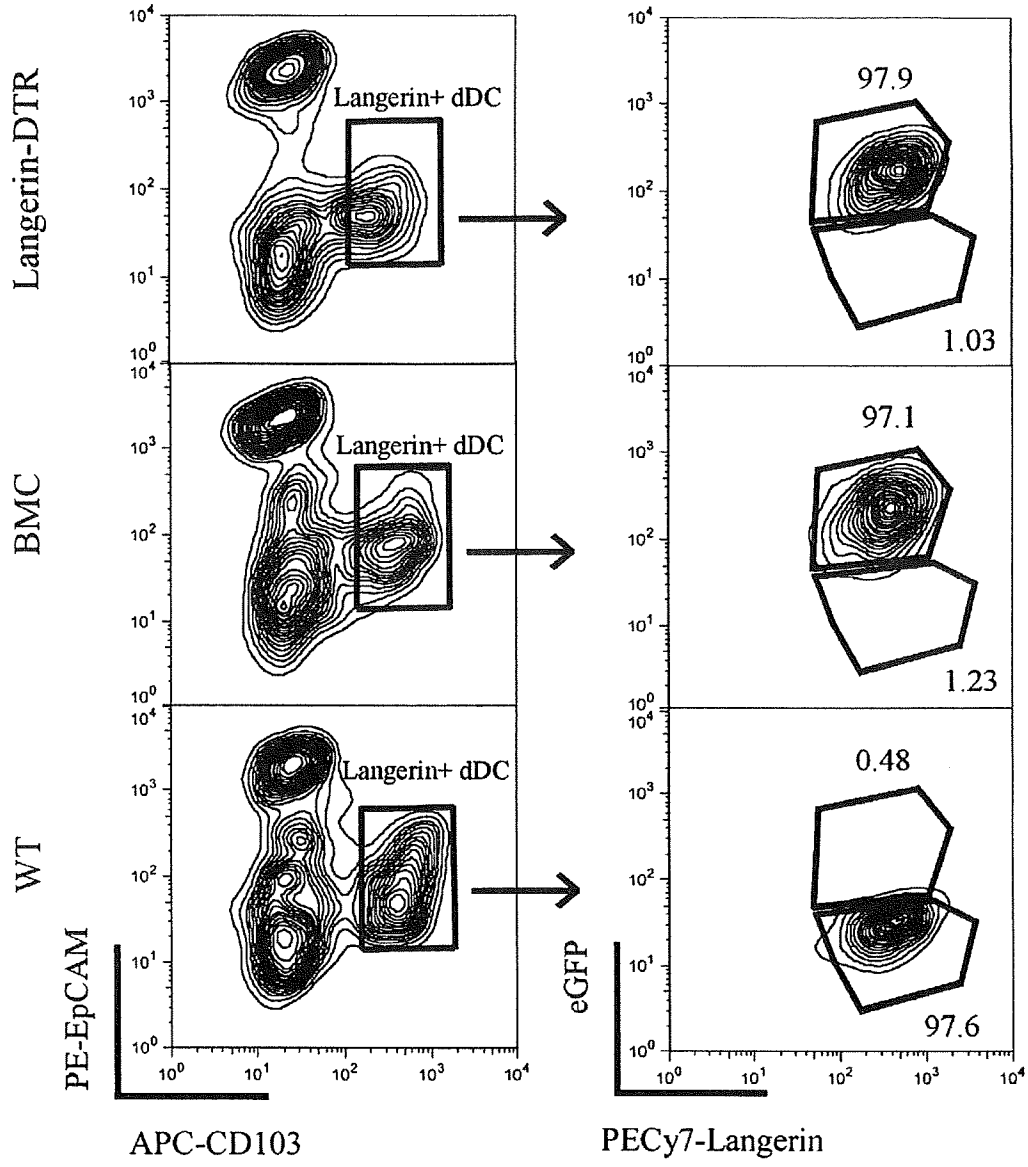

FIG E1. Chimerism of langerin-positive dDCs in BMC mice. The CD11c$^+$ MHC class II$^+$ EpCAM$^-$ CD103$^+$ langerin-positive DCs of the dermis from langerin-eGFP-DTR, BMC, or B6 mice *(left panels)* were analyzed by means of flow cytometry for the expression of GFP. The frequencies (percentages) of GFP$^+$ and GFP$^-$ cells among langerin-positive dDCs are shown *(right panels)*. *APC*, Allophycocyanin; *PE*, phycoerythrin; *PECy7*, phycoerythrin-Cy7; *WT*, Wild Type.

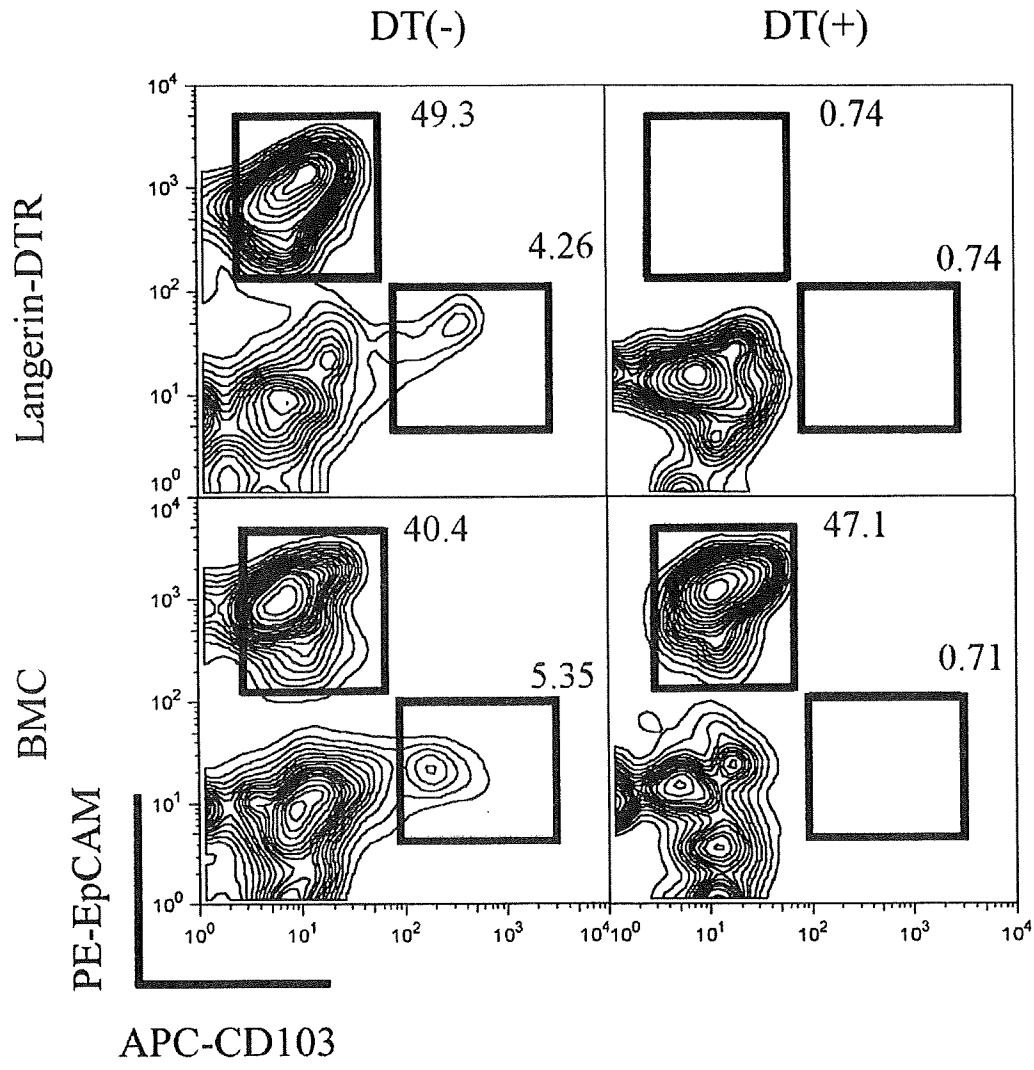

FIG E2. Effect of DT on reconstituted langerin-positive dDCs in BMC mice. Langerin-eGFP-DTR and BMC mice were treated with or without DT, and the CD11c$^+$ MHC class II$^+$ EpCAM$^-$ CD103$^+$ and CD11c$^+$ MHC class II$^+$ EpCAM$^+$ CD103$^-$ dDC subsets were analyzed by means of flow cytometry. The frequencies (percentages) of EpCAM$^+$ CD103$^-$ and EpCAM$^-$ CD103$^+$ cells among CD11c$^+$ MHC class II$^+$ DCs in the dermis are shown. *APC*, Allophycocyanin; *PE*, phycoerythrin.

ORIGINAL ARTICLE

Inducible Nitric Oxide Synthase Downmodulates Contact Hypersensitivity by Suppressing Dendritic Cell Migration and Survival

Kazunari Sugita[1], Kenji Kabashima[1,4], Ryutaro Yoshiki[1], Atsuko Ikenouchi-Sugita[2], Masato Tsutsui[3], Jun Nakamura[2], Nobuyuki Yanagihara[3] and Yoshiki Tokura[1]

Nitric oxide (NO) has several important roles in various physiological settings; one of the NO synthases, inducible NO synthase (iNOS), is induced by external stimulation of the skin. A prototypic example of external stimulation is hapten exposure, which induces the T-cell-mediated immune response known as contact hypersensitivity (CHS). We herein report on cutaneous dendritic cell (DC) function in the presence of an iNOS-specific inhibitor during the sensitization phase of CHS. First, we examined epidermal cell (EC) suspensions using flow cytometry with an iNOS antibody and confirmed that iNOS was expressed in the cytoplasm of Langerhans cells (LCs). We then studied the role of iNOS in CHS, and found that responses to DNFB were enhanced by the addition of an iNOS inhibitor during sensitization. Similarly, the iNOS inhibitor augmented FITC-induced migration of cutaneous DCs, including Langerin$^+$ LCs and Langerin$^-$ dermal DCs, to draining lymph nodes. Finally, we showed that iNOS inhibitor enhanced LC survival *in vitro*. We concluded that NO suppresses migration and survival of cutaneous DCs, resulting in a downmodulation of CHS.

Journal of Investigative Dermatology (2010) **130**, 464–471; doi:10.1038/jid.2009.288; published online 3 September 2009

INTRODUCTION

Inducible nitric oxide (NO) synthase (iNOS) is one of the three isoenzymes that generate NO from its precursor L-arginine. In the skin, keratinocytes (Arany *et al.*, 1996), Langerhans cells (LCs) (Qureshi *et al.*, 1996), dermal fibroblasts (Wang *et al.*, 1996), and melanocytes (Rocha and Guillo, 2001) express iNOS upon stimulation with inflammatory cytokines and/or lipopolysaccharide (LPS). Although NO can be proinflammatory when produced in large amounts, it may also regulate adaptive immune responses (Kuchel *et al.*, 2003). The best characterized example is the induction of iNOS by LPS and IFN-γ in murine macrophages (Lu *et al.*, 1996), LCs (Qureshi *et al.*, 1996), and keratinocytes (Yamaoka *et al.*, 2000). Although some information has thus been accumulated regarding the *in vitro* effects of iNOS on skin immunocompetent cells, the *in vivo* actions of iNOS remain unknown.

Murine contact hypersensitivity (CHS) is an antigen-specific immune response consisting of the two phases, namely, sensitization and elicitation. The constituents involved in its pathogenesis are Th1/Tc1 cells serving as helper/effector cells (Akiba *et al.*, 2002); cutaneous dendritic cells (DCs), including epidermal LCs and dermal DCs (dDCs), as antigen-presenting cells (Kissenpfennig and Malissen, 2006); and keratinocytes as a source of IL-1α, tumor necrosis factor-α, and GM-CSF to the LCs (Sugita *et al.*, 2007). iNOS is induced in LCs and keratinocytes by contact allergens; this supports the view that iNOS has a role in CHS (Morita *et al.*, 1996). It has previously been reported that an iNOS inhibitor injected intradermally during the elicitation phase suppressed CHS responses (Ross *et al.*, 1998), but the specificity of this iNOS inhibitor is not clear; furthermore, the role of iNOS in the sensitization phase remains unknown.

In this study, we investigated the effects of an iNOS-specific inhibitor in order to determine whether iNOS functions as a positive or negative regulator in CHS. Our results show that iNOS suppresses the CHS response by downmodulating the migration and survival of DCs.

RESULTS

iNOS inhibitor enhances CHS response to DNFB

First, we tested the degree of CHS response in mice treated with L-N^6-iminoethyl-lysine (L-NIL), an iNOS inhibitor.

[1]*Department of Dermatology, University of Occupational and Environmental Health, Kitakyushu, Japan;* [2]*Department of Psychiatry, University of Occupational and Environmental Health, Kitakyushu, Japan;* [3]*Department of Pharmacology, University of Occupational and Environmental Health, Kitakyushu, Japan and* [4]*Department of Dermatology, Kyoto University Graduate School of Medicine, Kyoto, Japan*

Correspondence: Dr K Sugita, Department of Dermatology, University of Occupational and Environmental Health, 1-1 Iseigaoka, Yahatanishi-ku, Kitakyushu 807-8555, Japan. E-mail: k-sugita@med.uoeh-u.ac.jp

Abbreviations: Ab, antibody; B6, C57BL/6; CCL21, CC chemokine ligand 21; CCR7, CC chemokine receptor 7; CHS, contact hypersensitivity; DC, dendritic cell; dDC, dermal DC; EC, epidermal cell; iNOS, inducible nitric oxide synthase; LC, Langerhans cell; L-NIL, L-N^6-iminoethyl-lysine; LPS, lipopolysaccharide; NO, nitric oxide; PBS, phosphate-buffered saline

Received 2 March 2009; revised 9 July 2009; accepted 19 July 2009; published online 3 September 2009

The mice were sensitized and challenged with DNFB, and their ear swelling responses were measured 24 hours after the challenge. A significantly higher degree of ear swelling response was observed in C57BL/6 (B6) mice treated intraperitoneally with L-NIL throughout the sensitization phase than in non-treated control mice (Figure 1a). Similar results were obtained 48 hours after the challenge (data not shown). In addition, histological analysis of the L-NIL-treated mice showed a remarkable infiltration of lymphocytes into the edematous dermis, which was not seen in untreated mice (Figure 1b). To confirm that L-NIL was biologically active in the skin when administered systemically, we measured the NOx ($NO_2^- + NO_3^-$) concentration of DNFB-sensitized skin. NOx production induced by DNFB was inhibited by an intraperitoneal injection of L-NIL (Supplementary Figure S1), suggesting that L-NIL is biologically active in lesional skin even when it is administered systemically.

iNOS expression in keratinocytes and LCs

Freshly isolated murine epidermal cells (ECs) were incubated for 24 hours in a culture medium, and the LCs and keratinocytes among them were analyzed for iNOS expression with flow cytometry. Both the keratinocytes and the LCs bore iNOS in the cytoplasm (Figure 2a). iNOS expression was greater in the mature LCs (major histocompatibility complex (MHC) class II high expression) than in the immature LCs (MHC class II intermediate expression). We carried out the same analysis on ECs that had been cultured for 24 hours in the presence of LPS, and found that LPS increased the number of LCs that highly expressed iNOS (Figure 2b).

iNOS inhibitor increases cutaneous DC accumulation in regional lymph nodes

To investigate the *in vivo* significance of iNOS for cutaneous DCs, we performed an FITC-induced cutaneous

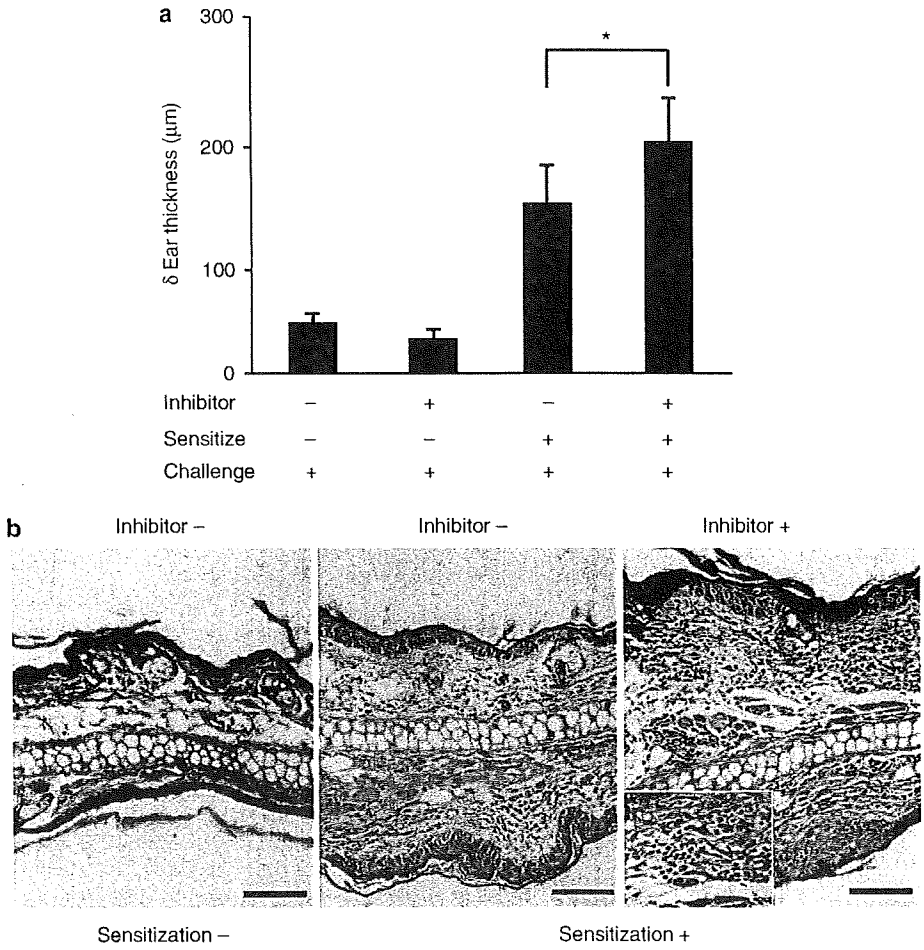

Figure 1. Increased CHS response to DNFB caused by blockade of iNOS. (**a**) For CHS model, B6 mice were immunized by the application of 0.5% DNFB to their shaved abdomens. They were challenged on both ears with 0.3% DNFB. iNOS inhibitor was applied through intraperitoneal injection (2.5 mg in 0.5 ml PBS twice daily). Ear thickness swelling was measured 24 hours later. Data are expressed as the mean ± SD of five mice. *$P<0.05$. (**b**) Non-sensitized ears, challenged ears, and challenged ears from non-treated mice (inhibitor –) were stained with hematoxylin and eosin. Inset: close-up view of hematoxylin and eosin staining of ears from mice treated with iNOS inhibitor, showing perivascular lymphocytic infiltration. Bar = 80 μm. Data are from three independent experiments.

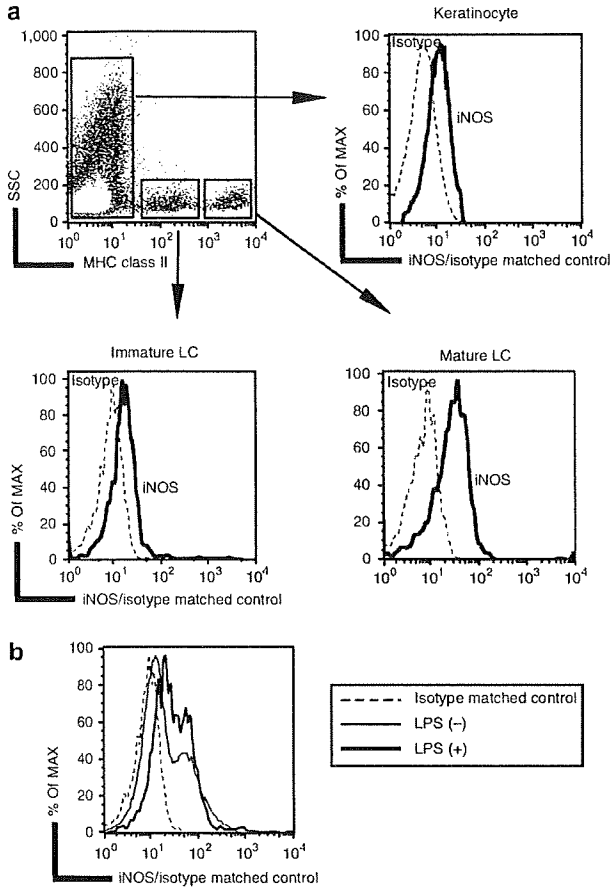

Figure 2. Expression of iNOS by both keratinocytes and LCs. (a) EC suspensions were analyzed for the expression of iNOS by means of flow cytometry. For intracellular detection of iNOS, cell fixation–permeabilization was performed before immunolabeling with anti-iNOS and anti-MHC class II mAbs. LCs or keratinocytes were gated by MHC class II positivity. (b) EC suspensions from naive mice were cultured with or without LPS (1 μg ml $^{-1}$) for 24 hours. The cultured cells were subjected to a flow cytometric analysis, which allowed us to measure the expression of iNOS. Data are from three independent experiments.

DC migration assay. FITC applied to the skin is taken up by cutaneous DCs, which subsequently migrate to the draining lymph nodes as FITC$^+$ MHC class II$^+$ cells. We intraperitoneally injected L-NIL, an iNOS inhibitor (2.5 mg in 0.5 ml phosphate-buffered saline (PBS) twice daily for 4 consecutive days) or the equivalent amount of PBS into mice; 24 hours after the last injection, we applied FITC to the abdomen. We then isolated axillary and inguinal draining lymph node cells 72 hours after FITC application and characterized the FITC$^+$MHC class II$^+$ cutaneous DCs therein by flow cytometry. Staining for Langerin showed that two subsets of the FITC$^+$ MHC class II$^+$ cutaneous DCs, the dDCs and LCs, were present in significantly greater numbers because of treatment with iNOS inhibitor (Figure 3a and b). Therefore, the blockade of iNOS promoted lymph node accumulation of cutaneous DCs in response to skin exposure to an antigen.

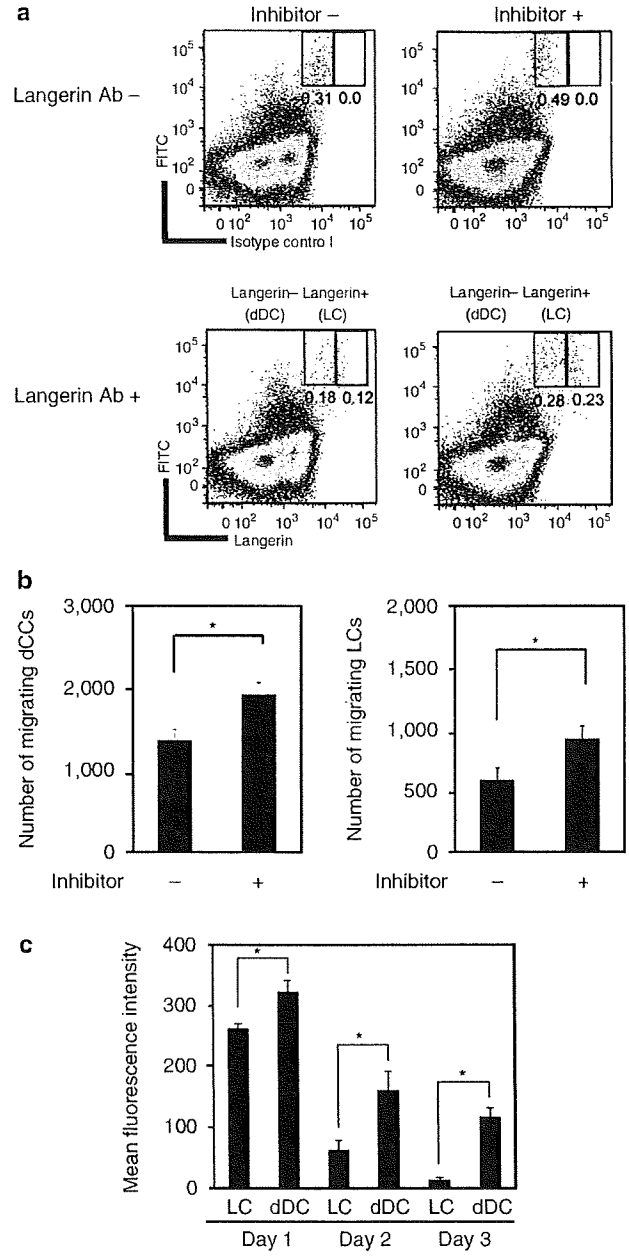

Figure 3. Augmented cutaneous DC accumulation in regional lymph nodes by iNOS blockade. (a) Langerin expression and FITC fluorescence in cells derived from regional lymph nodes were analyzed by means of flow cytometry 72 hours after the application of 200 μl of 2% FITC. The percentage of migrating LCs is indicated. (b) Migrating dDCs or LCs were counted 72 hours after FITC painting. Columns show the mean ± SD from at least four mice per group. *$P<0.05$. (c) Expression of iNOS in migrating LCs and dDCs. Draining lymph node cells were taken from mice painted with FITC on the abdomen and stained with anti-MHC class II, Langerin, and iNOS mAbs. Days 1, 2, and 3 indicate the number of days since FITC painting. Data are expressed as mean fluorescence intensity (MFI) for iNOS. MFI was the value of LCs or dDCs subtracted from that of the isotype-matched control. Columns show the mean ± SD. *$P<0.01$. Results are representative of three independent experiments.

iNOS expression in migrating LCs and dDCs

We examined iNOS expression in freshly isolated LCs and dDCs, both of which are capable of migrating into the lymph nodes on sensitization. The expression of iNOS in these cells was examined with FITC and anti-Langerin mAb. FITC was applied to the abdomen, and draining lymph node cells were sampled 24, 48, and 72 hours later. These cells were then labeled with anti-MHC class II mAb, anti-Langerin Ab, and anti-iNOS Ab. Although LCs are positive for Langerin, most dermal DCs are negative for Langerin (Nagao *et al.*, 2009), iNOS was present in both LCs and dDCs. The mean fluorescence intensity for iNOS was as follows: LC, 11.9 ± 4.1; dDC, 36.6 ± 20.5 (mean ± SD of three mice).

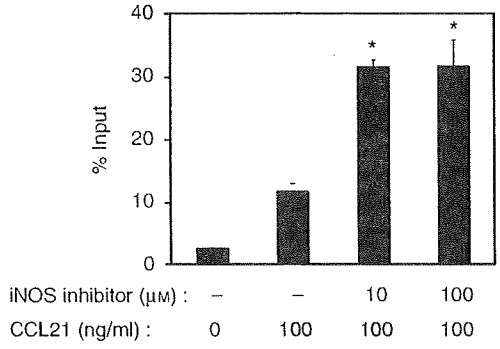

Figure 4. Chemotactic activity of epidermal LCs to CCL21. EC suspensions were incubated with or without iNOS inhibitor plus LPS in culture medium for 9 hours and applied to a transwell. CCL21 at 100 ng ml^{-1} was administered to the lower chamber. Migrating epidermal LCs in the lower chamber were identified as belonging to the MHC class II$^+$ subset. The number of migrating LCs was calculated. Columns represent the mean ± SD of triplicated transwells, and data are from three independent experiments. *$P<0.01$.

These data suggested that iNOS was weakly expressed only in freshly isolated LCs and dDCs, in amounts too small to be statistically significant. Nevertheless, we were able to observe that the dDCs showed a higher mean fluorescence intensity of iNOS expression than the LCs did (Figure 3c).

Chemotactic activity of LCs to CCL21

EC suspensions were incubated with LPS in a culture medium for 9 hours and applied to transwells in the presence or absence of L-NIL, an iNOS inhibitor. The migrating LCs in the lower chamber were identified as MHC class II$^+$ cells. CCL21 (CC chemokine ligand 21), a cytokine expressed in secondary lymphoid organs that mediates the chemotaxis of lymphocytes and DCs through its receptor, CCR7 (CC chemokine receptor 7; Saeki *et al.*, 1999), was then added to the lower chamber. All LCs exhibited a strong chemotactic response to this chemokine, but this response was significantly increased by the iNOS inhibitor (Figure 4).

iNOS inhibitor caused no alteration of the expression of co-stimulatory molecules or CCR7

The chemotaxis-promoting activity of the iNOS inhibitor, described above, raised the possibility that the iNOS inhibitor upregulates the expression of co-stimulatory molecules and CCR7. To determine whether this is the case, freshly isolated ECs were cultured for 24 hours in the presence or absence of the iNOS inhibitor, and the expression levels of these molecules were monitored by gating for MHC class II$^+$ LCs. After 24 hours of culture, a single population of LCs usually divides into two populations, with different expression levels of co-stimulatory molecules and CCR7 (Sugita *et al.*, 2007) (Figure 5a). The addition of the iNOS inhibitor did not alter the expression of CD86, CD80, CD40, or CCR7 (Figure 5a and b). In chemotaxis, however, the expression of

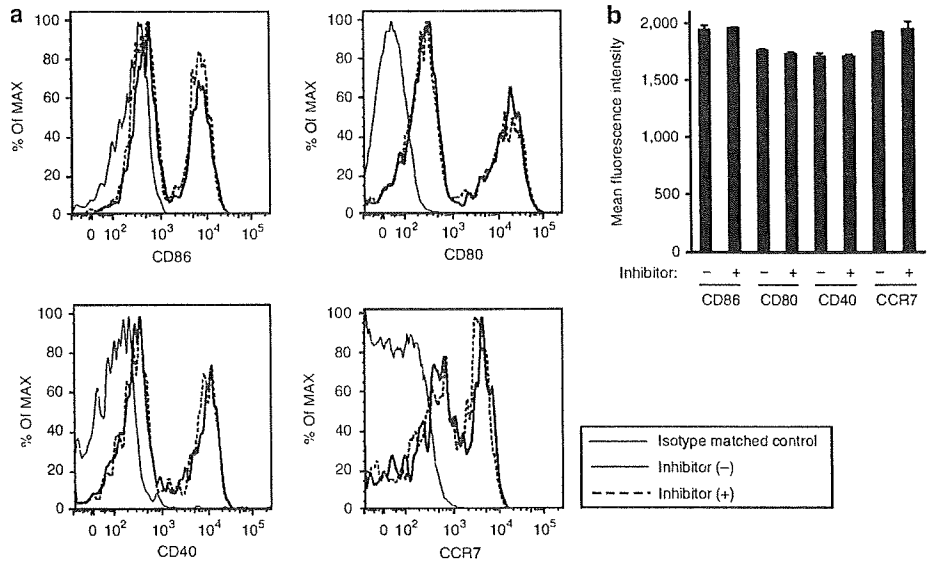

Figure 5. No modulation of CD86, CD80, CD40, or CCR7 expression in LCs by iNOS inhibitor. (**a** and **b**) EC suspensions from naive mice were cultured for 24 hours with or without iNOS inhibitor. The cultured LCs were examined for their expression levels of CD86, CD80, CD40, and CCR7. Data are representative of three independent experiments.

CCR7 in DCs is not sufficient to guarantee its functionality (Sanchez-Sanchez *et al.*, 2006); therefore, it is possible that iNOS alters certain downstream functions of LCs without affecting CCR7 expression.

iNOS inhibitor reduces LPS-induced apoptosis of LC

We then evaluated the effect of endogenous iNOS activity on the viability of LCs. EC suspensions from the earlobes of B6 mice were cultured for 9 hours with or without LPS in the presence or absence of L-NIL, an iNOS inhibitor. LPS stimulation reduced the number of LCs, but this reduction was reversed by the addition of the iNOS inhibitor (Figure 6a). It has been reported that epidermal LCs are unable to proliferate *in vitro* when they are incubated as an EC suspension (Schuler and Steinman, 1985), suggesting that the observed effects of the iNOS inhibitor stem from a survival change.

To examine whether the iNOS inhibitor promotes the survival of LCs, cellular viability was assessed through flow cytometry after Annexin V/propidium iodide staining and 9 hours of culture (Figure 6b). This flow cytometry experiment used anti-MHC class II and anti-CD11c mAbs. The percentage of Annexin V and propidium iodide double-positive cells in samples that had been treated with 100 μM iNOS inhibitor and those that had not was as follows: 100 μM, 1.6 ± 0.4%; no addition, 2.2 ± 1.0% (mean ± SD, $n = 3$). These results suggest that the reduction of apoptotic cells that occurs through iNOS inhibitor treatment is not due to the increment of necrotic cells. We found that LPS-induced apoptosis of LCs was reduced by the addition of the iNOS inhibitor (Figure 6c), suggesting that the iNOS inhibitor promotes DC survival.

DISCUSSION

The results of this study on the effects of an iNOS inhibitor include several major findings about the involvement of NO in the sensitization phase of CHS. First, CHS as a model of acquired skin immune response was enhanced by treatment with the iNOS inhibitor. Second, the iNOS inhibitor markedly increased the number of migrating cutaneous DCs. Accordingly, the chemotactic response of LCs to CCL21 was enhanced by *in vitro* incubation with the iNOS inhibitor. Finally, the iNOS inhibitor was capable of reducing LPS-induced apoptosis of LCs.

It has generally been believed that iNOS is involved in CHS as a producer of NO and a trigger of inflammatory responses (Cals-Grierson and Ormerod, 2004). It has been

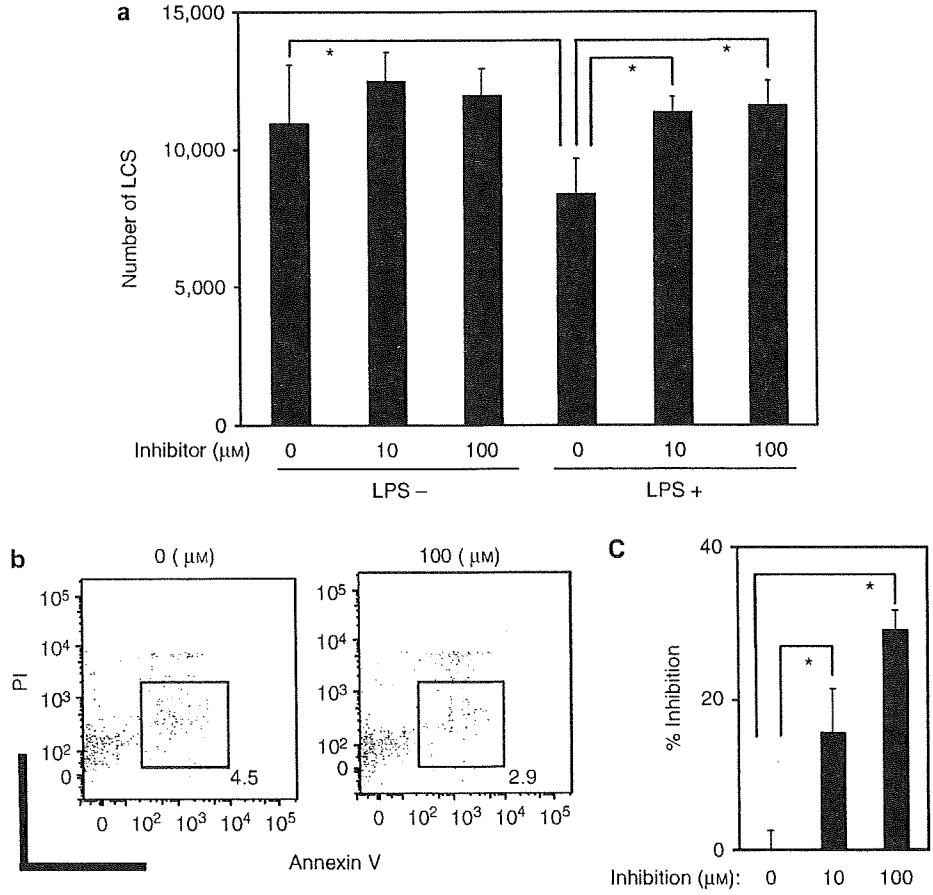

Figure 6. The effect of LPS on LC survival. (a) EC suspensions were cultured with or without LPS and iNOS inhibitor for 9–12 hours. iNOS inhibitor dose dependently increased the number of LCs. Columns show the mean ± SD. *$P<0.05$. Data are representative of three independent experiments. (b) Apoptosis was determined using annexin V/propidium iodide double staining. (c) The percentage inhibition is calculated. Data represent the mean ± SD. *$P<0.05$.

reported that iNOS and NO were produced in human skin subjected to positive patch tests to contact allergens (Cruz *et al.*, 2007; Ormerod *et al.*, 1997) and to the irritant sodium lauryl sulfate; nevertheless, it remains controversial whether iNOS is inhibitory or augmentative in CHS (Ross and Reske-Kunz, 2001). It has also been reported that an iNOS inhibitor exerted a suppressive effect on the CHS response to 2,4,6-trinitrochlorobenzene (TNCB) (Musoh *et al.*, 1998), although this effect was limited to the first few hours of the response, and neither NO production, NO-expressing cells, nor NOS isoenzymes were identified. Thus, the mode of action of iNOS in CHS remains a matter of debate.

It is possible that iNOS first modulates keratinocytes so that they produce cytokines, thereby subsequently modifying LC function. Yet, we found that the production levels of GM-CSF and tumor necrosis factor-α in the culture supernatant of primary keratinocytes of B6 mice cultured for 72 hours were not significantly affected by the presence of the iNOS inhibitor (Supplementary Figure S2). With regard to the effect of iNOS on T cells, we cultured immune $CD4^+$ T cells for 72 hours with varying concentrations of the iNOS inhibitor in the presence of anti-CD3 mAb and found that the iNOS inhibitor was incapable of stimulating T cells *per se* (Supplementary Figure S3).

LCs have traditionally been believed to have a role in the induction of CHS, but three research groups have reported three contradictory findings after applying haptens to transgenic mice deficient in LCs: a diminished reaction (Bennett *et al.*, 2005), an enhanced reaction (Kaplan *et al.*, 2005), and an unchanged response (Kissenpfennig *et al.*, 2005). Moreover, recent findings suggest that dDCs has a critical role in initiating CHS (Fukunaga *et al.*, 2008). In our study, dDCs augmented iNOS expression in response to hapten application more than LCs did. Our findings suggest that iNOS can suppress cutaneous DC migration and survival. Given that, in CHS, dDCs and LCs have positive and regulatory capacities, respectively, our findings on cutaneous DCs seem to be consistent with the observation that iNOS inhibitor induces an enhancement of CHS.

The findings of our study are clinically relevant in two respects. First, iNOS and NO exert immunosuppressive effects on cutaneous inflammation. In this context, the *in vivo* immunosuppressive effect of NO has also been shown in human studies (Kuchel *et al.*, 2003). Second, iNOS reduces cutaneous DC function and survival in the sensitization phase of CHS. The observation that NO directly reduces the number of LCs in the human epidermis supports our conclusion (Mowbray *et al.*, 2008).

MATERIALS AND METHODS

Animals and reagents

Female B6 mice were purchased from Japan SLC (Hamamatsu, Japan). All experiments were conducted on 8-week-old mice. The mice were maintained on a 12-hour light/dark cycle under a specific pathogen-free condition. All protocols were approved by the Institutional Animal Care and Use Committee of the University of Occupational and Environmental Health. L-NIL (a highly selective inhibitor of iNOS enzymatic activity) and LPS were obtained from Sigma-Aldrich (St Louis, MO). CCL21 was purchased from R&D Systems (Minneapolis, MN).

DNFB-induced CHS model

B6 mice were sensitized through the application of 25 μl of 0.5% (v/v) DNFB in 4:1 acetone/olive oil to their shaved abdomens on day 0. They were then challenged on both sides of each ear with 20 μl of 0.3% (v/v) DNFB. Ear thickness change was calculated as follows: (ear thickness 24 or 48 hours after challenge)−(ear thickness before challenge). iNOS was inhibited with L-NIL as described previously (Diefenbach *et al.*, 1998). Briefly, L-NIL was applied by intraperitoneal injection (2.5 mg in 0.5 ml PBS twice daily) for 6 consecutive days starting 1 day before sensitization. We chose his protocol because treatment with L-NIL at this concentration and frequency for 4-13 days is one of the most common methods of blocking *in vivo* activity of iNOS (Diefenbach *et al.*, 1998; Stallmeyer *et al.*, 1999).

EC preparation and culture

EC suspensions were prepared as described previously (Tokura *et al.*, 1994). Ears of naive mice were split along the plane of the cartilage, which was then removed together with the subcutaneous tissue. These specimens were incubated for 1 hour at 37 °C in a 0.2% solution of trypsin in PBS. After incubation, the epidermis was separated from the dermis and the separated epidermal sheets were rubbed to disperse the ECs in PBS supplemented with 10% fetal calf serum. The cells were filtered and washed twice in PBS. As a culture medium, RPMI-1640 (Sigma-Aldrich) was supplemented with 10% heat-inactivated fetal calf serum, 5×10^{-5} M 2-mercaptoethanol, 2 mM L-glutamine, 25 mM HEPES (4-(2-hydroxyethyl)-1-piperazineethanesulfonic acid), 1 mM nonessential amino acids, 1 mM sodium pyruvate, 100 U ml^{-1} penicillin, and 100 μg ml^{-1} streptomycin.

Preparation of dermal cell suspensions

Dermal cells were obtained from normal murine skin from which the epidermis had been removed. Samples were minced and incubated for 2 hours at 37 °C in RPMI-1640 medium (Invitrogen, Carlsbad, CA) supplemented with collagenase (2 mg ml^{-1}; Sigma-Aldrich), hyaluronidase (260 U ml^{-1}; Sigma-Aldrich), DNase (0.1 mg ml^{-1}; ICN, Costa Mesa, CA), and 10 mM HEPES (Sigma-Aldrich). The obtained cells were filtered through a 40-μm filter.

Flow cytometry

For flow cytometry, cells were plated at a density of 1×10^6 cells per well in 96-well U-bottomed plates (Falcon, BD Biosciences, San Jose, CA). Cells were then stained for 20 minutes on ice with mAbs in 25 μl of PBS containing 2% fetal calf serum, 1 mM EDTA, and 0.1% NaN_3, and washed twice with 200 μl of this buffer. Data were collected on a FACSCanto system (BD Biosciences) and analyzed with FlowJo software (TreeStar, San Carlos, CA). The mAbs used were as follows: FITC-conjugated anti-CD86 and Annexin V mAbs, PE-conjugated anti-CD80 and CD40 mAbs, PE-Cy5-conjugated anti-MHC class II mAb, APC-conjugated anti-CD11c mAb (all from BD Biosciences), and PE-Cy7-conjugated anti-CCR7 mAb (eBioscience, San Diego, CA). For detection of Langerin and iNOS, anti-Langerin Ab (eBioscience), PE-conjugated anti-iNOS Ab (Santa Cruz Biotechnology, Santa Cruz, CA), and PE-Cy5-conjugated streptavidin were